https://doi.org/10.5194/gmd-2020-233
Preprint. Discussion started: 10 August 2020

Geoscientific Model Development Discussions

Inclusion of a suite of weathering tracers in the cGENIE Earth System Model - muffin release v.0.9.10

Markus Adloff[1], Andy Ridgwell[1,2], Fanny M. Monteiro[1], Ian J. Parkinson[3], Alexander Dickson[4], Philip A. E. Pogge von Strandmann[5], Matthew S. Fantle[6], and Sarah E. Greene[7]

[1]BRIDGE (Bristol Research Initiative for the Dynamic Global Environment), School of Geographical Sciences, University of Bristol, Bristol, UK
[2]Department of Earth Sciences, University of California Riverside, Riverside, California, USA
[3]School of Earth Sciences, University of Bristol, Bristol, UK
[4]Department of Earth Sciences, Royal Holloway University of London, London, UK
[5]London Geochemistry and Isotope Centre (LOGIC), Institute of Earth and Planetary Sciences, University College London and Birkbeck, University of London, London, UK
[6]Department of Geosciences, Penn State University, Pennsylvania, USA
[7]School of Geography, Earth and Environmental Sciences, University of Birmingham, Birmingham, UK

Correspondence: Markus Adloff (markus.adloff@bristol.ac.uk)

Abstract. The metals strontium (Sr), lithium (Li), osmium (Os) and calcium (Ca) and their isotopes are important tracers in the study of changes in weathering rates and volcanism, two main processes which shape the long-term cycling of carbon and other biogeochemically important elements at the Earth's surface. Traditionally, isotopic shifts of these four elements in the geologic record are interpreted with isotope-mixing, tracer-specific box models because of their long residence times in the ocean. However, these models often lack mechanistic links between the cycling of the four metals and other geochemically relevant elements, particularly carbon. Here we develop and evaluate the implementation of Sr, Li, Os and Ca isotopes into the Earth system model cGENIE. The model has the potential to study these metal systems at equilibrium and under perturbations alongside other biogeochemical cycles. We provide examples of how to apply this new model to investigate Sr, Li, Os and Ca isotope dynamics and responses to environmental change.

1 Introduction

The evolution of life and climate on Earth is intrinsically linked to the dynamics of carbon, oxygen and nutrients at the Earth's surface. While complex interactions on a range of spatial and temporal scales determine the distribution of these elements between surficial (non-lithological) reservoirs like oceans, atmosphere, biomass and soils, the total amount and isotopic distribution of these elements are ultimately governed by the balance between crust weathering, marine sediment deposition and mantle inputs during oceanic crust formation. Geological records show that the abundance of these elements at Earth's surface varied on time scales of thousands to millions of years. For example, the changing composition of mantle fluxes into the ocean and nutrient supply during weathering of large mountain ranges were potentially drivers of the accumulation of surficial oxygen during the Archean and Proterozoic (e.g. Kump and Barley, 2007; Campbell and Allen, 2008). Likewise, the supply of partic-

https://doi.org/10.5194/gmd-2020-233
Preprint. Discussion started: 10 August 2020


Geoscientific Model Development Discussions

ulate iron from airborne grounded rock to the oceans of the Quaternary is invoked as a mechanism to drive glacial-interglacial carbon cycle dynamics (e.g Martin, 1990; Martínez-Garcia et al., 2011; Loveley et al., 2017; Hooper et al., 2019). The emplacement of large igneous provinces (LIPs) repeatedly led to climatic and biotic crises by increasing the supply of mantle-derived carbon and nutrients to the oceans, e.g. during oceanic anoxic events (e.g. Erba et al., 2010; Jenkyns, 2010; Bottini et al., 2012; Monteiro et al., 2012; Percival et al., 2015). Increased basalt weathering in the Cenozoic could have led to a continuous decline in CO_2 concentrations, contributing to the reconstructed long-term cooling trend (e.g. Kent and Muttoni, 2013; Mills et al., 2014). Mass fluxes between the lithosphere and Earth's dynamic surface are thus important drivers of environmental processes on the Earth's surface over geological time scales, but our ability to measure these fluxes directly is limited by their long evolution times and large spatial extents. Instead, records of variations in the content and isotopic composition of trace metals like strontium (Sr), osmium (Os), lithium (Li) and calcium (Ca), preserved in marine sediments, are used to study lithological processes. The dynamics of these metals are controlled by processes that also shape the long-term carbon and nutrient cycles, namely continental and oceanic weathering and direct mantle emissions, but variations in their isotopic compositions can be linked more directly to changes in these processes since radioactive decay and mass-dependent fractionation form isotopically distinct lithological metal reservoirs. The residence time of these metals in the ocean is generally assumed to be greater than the mixing time of the ocean and therefore their distribution is comparably homogeneous (e.g. Faure and Mensing, 2005). While laboratory methods to measure and reconstruct the evolving trace metal composition of seawater have become increasingly precise, our ability to interpret these records is limited by our incomplete mechanistic understanding of the cycling of these metals and their isotopes. Quantifying reservoir sizes and fluxes constitute particular challenges under varying chemical conditions and marine productivity over geological time. Mass balances and box models have been most commonly used to interpret geological records of trace metal variations (e.g. Tejada et al., 2009; Misra and Froelich, 2012; Kristall et al., 2017; Them et al., 2017). They however rely on assumed fluxes and residence times based on today's ocean which might not always be applicable throughout the geological record.

Mechanistic Earth system models are useful tools to test our conceptual and mathematical understanding of processes against observations, and to explore characteristics and processes of biogeochemical cycling beyond modern observational data. The Earth system model of intermediate complexity cGENIE has been used successfully to study marine biogeochemical cycles (including C and Ca) under various boundary conditions and external forcings (e.g. Ridgwell and Zeebe, 2005; Ridgwell et al., 2007; John et al., 2014; Death et al., 2014; Turner and Ridgwell, 2016; Hülse et al., 2019). Implementing isotope enabled cycling of Sr, Os, Li and Ca in cGENIE allows us to test the influence of different assumptions about source and sink mechanisms, and efficiencies, on metal distributions in the ocean and their behaviour under environmental perturbations.

Here, we present our implementation of the marine cycling of Sr, Os, Li and Ca in cGENIE. We evaluate the model's performance by comparing simulations of pre-industrial trace metal distributions in the oceans to seawater measurements, and study their equilibration times to imposed geochemical perturbations compared to estimated seawater residence times for these elements.

https://doi.org/10.5194/gmd-2020-233
Preprint. Discussion started: 10 August 2020

Geoscientific Model Development Discussions

2 Observational constraints

We first provide a brief review of the systematics of Sr, Os, Li and Ca cycling in the ocean, as well as their observed concentrations and isotopic compositions. This discussion provides the theoretical basis for our model implementation, and the data compilations for the model evaluation at the end of this study.

2.1 Strontium

Of the four metals modelled in this study, Sr has the second highest marine concentration (3 – 4 times more abundant than Li and more than one billion times more abundant than Os, Broecker and Peng, 1982). The main source for marine Sr is continental weathering, replenishing the ocean reservoir through rivers and potentially groundwater discharge (Basu et al., 2001; Beck et al., 2013). Smaller sources are hydrothermal input of mantle-derived Sr and refluxes from diagenetic alteration of carbonates at the sea floor. The chemical and physical similarity of Sr to Ca leads to its substitution in aragonite and, to a lesser degree, calcite (Fietzke and Eisenhauer, 2006; Rüggeberg et al., 2008; Böhm et al., 2012; Stevenson et al., 2014). Angino et al. (1966) argue that biological uptake is the dominant driver of spatial gradients in Sr concentrations in today's oceans, and Krabbenhöft et al. (2010) predict that marine carbonate burial could be the most important sink of seawater Sr. The concentration of Sr incorporated into biogenic carbonates depends on the mineralogy and the growth rate with higher Sr/Ca ratios in aragonite precipitated at fast growth rates (Rickaby et al., 2002; Stevenson et al., 2014). By contrast, direct effects of temperature on elemental fractionation during the formation of calcite, the major carbonate buried in marine sediments, are small (Tang et al., 2008). Assuming rivers to be the only supply of continental Sr to the oceans, Hodell et al. (1989) estimates the marine residence time of Sr to be 1.9 – 3.45 Myr. Considering the potentially appreciable Sr influx from groundwater, the actual residence time might be at or below the lower end of this estimate.

Strontium has four stable isotopes (0.56% ^{84}Sr, 9.87% ^{86}Sr, 7.04% ^{87}Sr, 82.53% ^{88}Sr) (Veizer, 1989), although ^{87}Sr is also the product of β-decay of ^{87}Rb (half-life $4.88 \cdot 10^{10}$ yr (Faure and Mensing, 2005). Radiogenic Sr isotope ratios are reported as ^{87}Sr/^{86}Sr ratios whereas stable Sr isotope ratios are reported as $\delta^{88/86}$Sr, which is the per mille (‰) deviation in the ^{88}Sr/^{86}Sr relative to the NBS987 standard ($\delta^{88/86}\text{Sr} = (\frac{(^{88}\text{Sr}/^{86}\text{Sr})_{sample}}{(^{88}\text{Sr}/^{86}\text{Sr})_{std}} - 1) \cdot 1000$, Fietzke and Eisenhauer, 2006). Elemental fractionation during magmatic processes creates different Rb/Sr ratios that over time generate reservoirs with distinct Sr isotopic signatures with the continental crust being considerably more radiogenic than the mantle (Faure and Mensing, 2005). Dust and rainwater isotopic signatures, both radiogenic and stable, are generally lower than modern day seawater values (Pearce et al., 2015). Volcanic material brings unradiogenic particulate Sr into sediments and can over time significantly affect the radiogenic composition of dissolved Sr in the sediment column while having little effect on the isotopic composition of dissolved Sr in seawater (Elderfield and Gieskes, 1982; Pearce et al., 2015). Changes in isotope abundances caused by kinetic and mass-dependent fractionation during carbonate formation are much smaller, and one can thus assume that the ^{87}Sr/^{86}Sr of seawater and deposited carbonates is only controlled by inputs to the ocean (Krabbenhöft, 2011). By contrast, variations in $\delta^{88/86}$Sr are only controlled by fractionation during chemical processes, biogenic carbonate formation being the most important one in the ocean (e.g. Krabbenhöft et al., 2010). There is no evidence for a generic dependence of $\delta^{88/86}$Sr fractionation during

https://doi.org/10.5194/gmd-2020-233
Preprint. Discussion started: 10 August 2020

Geoscientific Model Development Discussions

biogenic carbonate formation on environmental conditions, although temperature and growth rate effects were observed in some calcifying species (Fietzke and Eisenhauer, 2006; Böhm et al., 2012; Stevenson et al., 2014; Vollstaedt et al., 2014).

Table 1. Estimates of pre-industrial Sr fluxes between surface reservoirs and their isotopic composition.

Process	Flux (Gmol/yr)	$^{87}Sr/^{86}Sr$	$\delta^{88/86}Sr$ (‰)	Reference
hydrothermal input flux	3-4	0.7035-0.70387	0.328-0.422	Pearce et al. (2015); Kristall et al. (2017)
input from diagenesis	3-5	0.7035-0.7084	0.27	Kristall et al. (2017)
dissolved riverine input	20.2-47	0.7111-0.7136	0.32	Allègre et al. (2010) Peucker-Ehrenbrink et al. (2010) Pearce et al. (2015); Kristall et al. (2017)
particulate riverine input	5.2	<0.7136	uncertain	Allègre et al. (2010) Peucker-Ehrenbrink et al. (2010) Kristall et al. (2017)
groundwater discharge	7.1-16.6	0.7089	0.354 ± 0.028	Basu et al. (2001); Beck et al. (2013)
dust flux and rainwater	uncertain	0.7075 - 0.7191	0.05 - 0.31	Pearce et al. (2015)
pelagic Sr burial in carbonates	12.5 - 174	seawater	0.20	Krabbenhöft et al. (2010) Stevenson et al. (2014) Kristall et al. (2017)
neritic Sr burial in carbonates	19	seawater	0.21	Krabbenhöft et al. (2010)
Sr burial in sea floor alteration	uncertain	seawater	seawater	Menzies and Seyfried Jr (1979) Kristall et al. (2017)

2.2 Osmium

Osmium is a siderophile and chalcophile element which led to its accumulation in the Earth's core (Goldschmidt, 1922) and is also compatible during mantel melting. As a result, it is one of the rarest elements in the Earth's crust and the oceans. Because of its low concentrations, the ability to measure Os in seawater only developed in the past few decades, limiting the number of observations of marine Os concentrations and isotopic compositions.

The cycling of Os at the Earth's surface is similar to that of radiogenic Sr in many aspects. Oxidative weathering of sediments is currently the most important natural source of Os to the oceans (Peucker-Ehrenbrink and Ravizza, 2000; Lu et al., 2017). The estimated annual input of such Os to the oceans via aeolian and riverine transport and groundwater discharge is about 5 times larger than all other natural inputs combined (Lu et al., 2017). Hydrothermal inputs constitute the next biggest source of oceanic Os with high and low temperature systems being of roughly equal importance (Georg et al., 2013). The high temperature hydrothermal source can be split into a basaltic and a peridotitic source (Burton et al., 2010). Unlike for Sr, cosmic and terrestrial dust are significant sources of marine Os, as well as volcanic aerosols, though field observations do not

https://doi.org/10.5194/gmd-2020-233
Preprint. Discussion started: 10 August 2020

Geoscientific Model Development Discussions

suggest that the latter significantly contributes to the oceanic inventory (Sharma et al., 2007). Os is removed from the ocean by deposition at the seafloor, predominantly under suboxic water masses and in ferro-manganese nodules (Lu et al., 2017). Os incorporation into biogenic carbonates constitutes an additional minor sink (Burton et al., 2010). The marine residence time of Os is inherently uncertain given the uncertainty in Os fluxes, although estimates range from 3 – 50 kyr (Sharma et al., 1997; Levasseur et al., 1998; Oxburgh, 2001).

Os has seven naturally occuring isotopes (0.02% ^{184}Os, 1.59% ^{186}Os, 1.51% ^{187}Os, 13.29% ^{188}Os, 16.22% ^{189}Os, 26.38% ^{190}Os, 40.98% ^{192}Os). ^{186}Os has such a long half-life that it can also be treated as stable over geological times, whereas ^{187}Os is radiogenic due to the beta decay of ^{187}Re (Faure and Mensing, 2005). The isotopic composition of Os in marine sediments provides insight into changing fluxes between different Os reservoirs, particularly weathering related Os fluxes from the continents and mantle derived fluxes from volcanic activity. During partial melt in the upper mantle Os is compatible and rhenium (Re) is incompatible, leading to an increased Re/Os ratio in continental crust relative to the mantle (Dąbek and Halas, 2007), and therefore elevated ^{187}Os/^{188}Os ratios in the continental crust compared to the mantle. No mass-dependent fractionation has been observed during Os uptake into macroalgae (Racionero-Gómez et al., 2017) and is not assumed to occur during other fluxes between surface reservoirs.

Table 2. Estimates of pre-industrial Os fluxes between surface reservoirs and their isotopic composition.

Process	flux estimate (kg/yr)	^{187}Os/^{188}Os	reference
riverine input (corrected for estuaries)	267-284	1.2-1.5	Sharma et al. (2007); Georg et al. (2013)
groundwater discharge	182	1.2-1.5	Lu et al. (2017)
terrogenous and cosmic dust	35-88	0.12-0.60	Lu et al. (2017)
high-temperature hydrothermal input	30	0.13	Sharma et al. (2007); Georg et al. (2013)
low-temperature hydrothermal input	19-56	0.88	Sharma et al. (2007); Georg et al. (2013)
burial in biogenic carbonates	4-5.3 ppt Os/Ca	seawater	Burton et al. (2010)
oxic burial in marine sediments	2-372	seawater	Lu et al. (2017)
suboxic burial in marine sediments	458-2802	seawater	Lu et al. (2017)

2.3 Lithium

Lithium is the 25th most abundant element in the Earth's crust, and it is more concentrated in continental crust than in oceanic crust (Baskaran, 2011). Weathering, in particular of silicate rocks, releases dissolved Li to rivers and soils where it is partially bound during clay formation (Kısakűrek et al., 2005; Dellinger et al., 2015; Pogge von Strandmann et al., 2017). The remaining dissolved Li is transported to the oceans via rivers and groundwater. Aeolian transport only contributes a minor flux of Li to the oceans (Baskaran, 2011). Li is also added to the oceans by hydrothermal vents and submarine weathering, but the size of this flux is more uncertain (Chan et al., 1992; Hathorne and James, 2006). Removal from the ocean happens predominantly via Li adsorption onto clay minerals, with a minor proportion buried with Li-containing biogenic calcite (Hathorne and James, 2006). These removal fluxes are dependent on the abundance of inorganic carbon and pH (Hall and Chan, 2004; Marriott et al.,

https://doi.org/10.5194/gmd-2020-233
Preprint. Discussion started: 10 August 2020

Geoscientific Model Development Discussions

2004), and are not uniform (Hathorne and James, 2006). The residence time of Li in the ocean is estimated to be 0.3 – 3 Ma (Stoffyn-Egli and Mackenzie, 1984) with more recent estimates closer to 1 Ma (Vigier and Goddéris, 2015).

Li has two stable isotopes (7.52% ^{6}Li and 92.48% ^{7}Li, Penniston-Dorland et al., 2017). Changes in the abundance of Li isotopes on Earth are related to mass-dependent fractionation processes. The isotopic composition of Li is expressed as δ^7Li, which is the ‰ deviation of the ^{7}Li/^{6}Li ratio from the L-SVEC standard ($\delta^7\text{Li} = (\frac{(^7\text{Li}/^6\text{Li})_{sample}}{(^7\text{Li}/^6\text{Li})_{std}} - 1) \cdot 1000$). While earlier studies suggest considerable variation in seawater δ^7Li (Carignan et al., 2004), recent studies suggest that seawater is remarkably homogeneous in its δ^7Li (Hall et al., 2005; Rosner et al., 2007; Penniston-Dorland et al., 2017) consistent with its long residence time. Mass-dependent isotope fractionation has been observed during clay formation, adsorption onto minerals and incorporation of Li into calcite shells (Pistiner and Henderson, 2003; Rudnick et al., 2004; Dellinger et al., 2015; Hindshaw et al., 2019), while kinetic fractionation occurs in magmatic systems due to diffusion (Parkinson et al., 2007; Penniston-Dorland et al., 2017), and potentially in aqueous solutions (Richter et al., 2006). Isotopic differences in weathered lithologies and post-weathering formation of secondary minerals in rivers and soils result in a large spatial and temporal variability of the δ^7Li of continental run-off (Huh et al., 1998; Pistiner and Henderson, 2003; Pogge von Strandmann and Henderson, 2015). Temporal variations in the amount of secondary mineral formation on land have the potential to drive shifts in seawater δ^7Li over geological time (Misra and Froelich, 2012; Pogge von Strandmann and Henderson, 2015). Fractionation during biogenic carbonate formation results in carbonate δ^7Li values that are a few ‰ lower than seawater, but this offset seems to be carbonate producer-dependent Hathorne and James (2006).

Table 3. Estimates of pre-industrial Li fluxes between surface reservoirs and their isotopic composition.

Process	flux estimate (Gmol yr^{-1})	δ^7Li (‰)	reference
continental run-off	8-16	23	Hathorne and James (2006); Misra and Froelich (2012)
hydrothermal vents	3-15	8.3	Hathorne and James (2006); Misra and Froelich (2012)
subduction reflux	6	15	Misra and Froelich (2012)
loss to sea spray	0.1	sea water	Stoffyn-Egli and Mackenzie (1984)
secondary mineral formation	3.5-37	16	Hathorne and James (2006); Misra and Froelich (2012)
sea floor alteration	1-12	16	Hathorne and James (2006); Misra and Froelich (2012)
neritic carbonate burial	1.7 - 81.3 μmol/mol Li/Ca	20 - 40	Rollion-Bard et al. (2009); Dellinger et al. (2018)
pelagic carbonate burial	10.4 - 14.5 μmol/mol Li/Ca	27.1 - 31.4	Hathorne and James (2006)

2.4 Calcium

Calcium cycling is closely linked to the C cycle, both shaping and shaped by the size of C reservoirs and C fluxes at the Earth's surface. Similar to Sr, Os and Li, the dominant Ca source for today's oceans is weathering-derived dissolved and particulate Ca in continental runoff. Input through hydrothermal vents near ocean ridges is on the order of 20% of the riverine flux (e.g. Milliman, 1993; DePaolo, 2004). Unlike Sr, Os, and Li, Ca plays an important role in many biological systems, predominantly as an electrolyte and building block for biogenic minerals (e.g. shells, exoskeletons, bones and teeth). In the ocean, Ca ions are

https://doi.org/10.5194/gmd-2020-233
Preprint. Discussion started: 10 August 2020

Geoscientific Model Development Discussions

incorporated into biogenic minerals (e.g. foraminiferal tests and calcareous nannoplankton), or form hydrogenetic or authigenic minerals (Fantle et al., 2020) if waters are highly saturated (Ω=$a_{Ca^{2+}} \cdot a_{CO_3^{2-}}/K_{sp}$). The resulting minerals are dissolved in undersaturated conditions, or buried, compacted, and lithified. Carbonate formation creates the biggest long-term Ca and C sinks in today's oceans, and marine carbonate accumulation and dissolution constitute a significant buffer mechanism to stabilize marine and atmospheric pCO_2 during periods of enhanced exogenic C input. The residence time of Ca in seawater is estimated to be 0.5-1.3 million years (Milliman, 1993; Sime et al., 2007; Griffith et al., 2008).

Ca has 6 stable isotopes (96.941% ^{40}Ca, 0.647% ^{42}Ca, 0.135% ^{43}Ca, 2.086% ^{44}Ca, 0.004% ^{46}Ca, 0.187% ^{48}Ca). ^{48}Ca has such a long half-life time that it can be treated as a stable isotope, whereas a small component of the ^{40}Ca in a rock mineral is radiogenic (via decay of ^{40}K; $t_1/2$= 1.248 Ga) and accumulates in continental crust over geological time scales (Fantle and Tipper, 2014). The isotopic composition of Ca is reported as either $\delta^{44/40}$Ca or $\delta^{44/42}$Ca, which are the ‰ deviations in $\delta^{44/40}$Ca and $\delta^{44/42}$Ca, respectively, from NIST SRM-915a, SRM-915b, or modern seawater (see Fantle and Tipper, 2014, for discussion): ($\delta^{44/40}$Ca = $(\frac{(^{44}Ca/^{40}Ca)_{sample}}{(^{44}Ca/^{40}Ca)_{std}} - 1) \cdot 1000$ and $\delta^{44/42}$Ca = $(\frac{(^{44}Ca/^{42}Ca)_{sample}}{(^{44}Ca/^{42}Ca)_{std}} - 1) \cdot 1000$). We use the $\delta^{44/40}$Ca notation in this study, from now on shortened to δ^{44}Ca, with NIST SRM-915a as standard. Dissolution of carbonates and silicates, as well as the precipitation of secondary silicate minerals controls the Ca isotopic composition in soil pore fluids, lakes and rivers (Farkaš et al., 2007; Tipper et al., 2008; Hindshaw et al., 2013; Fantle and Tipper, 2014; Kasemann et al., 2014; Perez-Fernandez et al., 2017). Both, biotic and abiotic precipitation of carbonates fractionate Ca isotopically, generating minerals with low δ^{44}Ca values relative to aqueous Ca^{2+}. The isotopic fractionation factor is most strongly a function of precipitation rate (and thus and solution chemistry, e.g. DePaolo, 2011) and is close to one ($\Delta \sim 0$) in the marine sedimentary column (see reviews in Blättler et al., 2012; Fantle and Tipper, 2014). In the ocean, species-dependent fractionation has been observed for several groups of calcifiers, with a small dependence on temperature (e.g. Nägler et al., 2000).

Table 4. Estimates of pre-industrial Ca fluxes between surface reservoirs and their isotopic composition. $\delta^{44/40}$Ca are given relative to NIST SRM915a (offset by +1.8825±0.07 from seawater (Holmden et al., 2012))

Process	flux (Tmol yr^{-1})	$\delta^{44/40}$Ca (‰)	reference
hydrothermal input flux	2-20	0.93±0.05	Berner and Berner (2012); Zhu and Macdougall (1998) Holmden et al. (2012); Tipper et al. (2016)
input from diagenesis	0.92	0.6±0.77	Berner and Berner (2012); Fantle and Tipper (2014)
riverine input	13.72	0.88±0.5	Berner and Berner (2012); Holmden et al. (2012) Fantle and Tipper (2014)
groundwater discharge	5.24 - 13.22	0.58 - 0.85±0.23	Berner and Berner (2012); Holmden et al. (2012) Fantle and Tipper (2014)
dust flux	0.05 - 2.25	0.72±0.6	Fantle et al. (2012); Fantle and Tipper (2014)
Ca burial in carbonates	23.95 - 31.94	0.58 - 0.78	Holmden et al. (2012); Fantle and Tipper (2014)

https://doi.org/10.5194/gmd-2020-233
Preprint. Discussion started: 10 August 2020

Geoscientific Model Development Discussions

2.5 Metal distributions in seawater

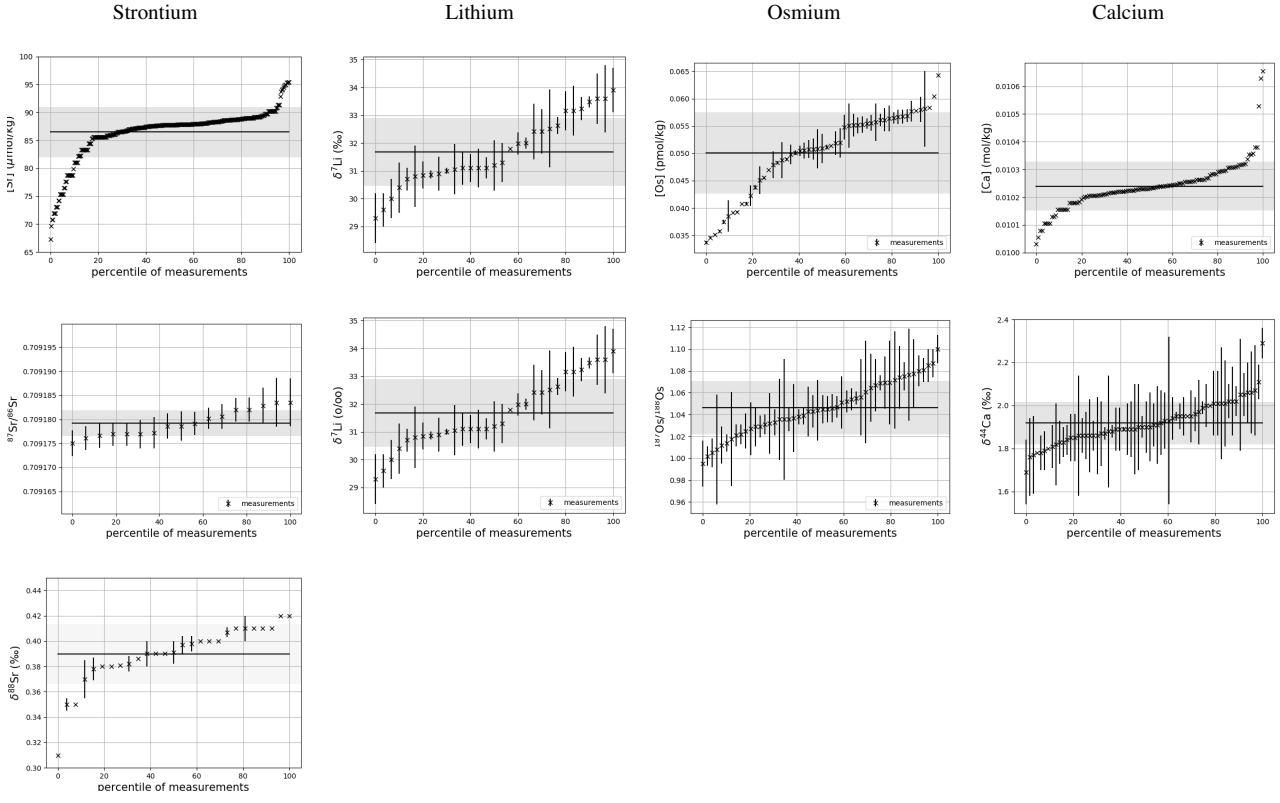

Figure 1. Sr, Li, Os and Ca contents of seawater. Shown are composites of all published measured concentrations and isotope ratios with reported errors. From these, we calculated mean concentrations and isotope ratios which are indicated by horizontal lines. Shading indicates one standard deviation around the means. Data are taken from Angino et al. (1966), Fabricand et al. (1967), Bernat et al. (1972), Brass and Turekian (1974), De Villiers (1999), Pearce et al. (2015), Mokadem et al. (2015) and the compilation of Wakaki et al. (2017) for Sr, Angino and Billings (1966), Fabricand et al. (1967), Chan (1987), Chan and Edmond (1988), You and Chan (1996), Moriguti and Nakamura (1998), Tomascak et al. (1999), James and Palmer (2000), Košler et al. (2001), Nishio and Nakai (2002), Hall, Bryant et al. (2003), Pistiner and Henderson (2003), Millot et al. (2004), Choi et al. (2010), Pogge von Strandmann et al. (2010), Phan et al. (2016), Lin et al. (2016), Henchiri et al. (2016), Weynell et al. (2017), Fries et al. (2019), Gou et al. (2019), Hindshaw et al. (2019), Murphy et al. (2019) and Pogge von Strandmann et al. (2019) for Li, Levasseur et al. (1998), Woodhouse et al. (1999) and Gannoun and Burton (2014) for Os and Fabricand et al. (1967), De Villiers (1999) and Fantle and Tipper (2014) for Ca.

Dissolved Sr, Os, Li and Ca are largely homogeneous in sea water, which is illustrated in figure 1 by sorting all seawater measurements - independent of location and depth - by their measured value. Measurements of a perfectly homogeneous seawater property would appear as a horizontal line in this plot, since the same value would be measured everywhere in the ocean. Most

https://doi.org/10.5194/gmd-2020-233
Preprint. Discussion started: 10 August 2020


Geoscientific Model Development Discussions

trace metal measurements have a difference of less than one standard deviation from the respective mean, suggesting very small spatial heterogeneities. In particular, most measured isotopic compositions are analytically indistinguishable from the standard deviation of the overall data population. Larger differences between lowest and highest measured metal concentrations indicate heterogeneity (potentially horizontal and/or vertical gradients) in metal abundances or are an artefact of the small number of sub-surface measurements. One possible example is Sr, which is reportedly less abundant in surface waters and waters in the North Atlantic than in deeper waters and sites outside the North Atlantic (see fig. A1). Higher Li concentrations in the surface ocean compared with deeper waters are only reported in one study, Angino and Billings (1966), while no vertical gradients are apparent in Fabricand et al. (1967) and Hall. These differences suggest that the spread in Li concentrations in fig. 1 could be the result of analytical uncertainty rather than real gradients in dissolved Li. Os concentrations vary between sites, but only a few sub-surface measurements are available and there is considerable variation in Os concentration between measurement techniques (Gannoun and Burton, 2014). Ca profiles show no apparent spatial patterns.

2.6 Application of Sr, Os, Li and Ca isotopes as proxies of weathering and mantle emissions

The isotopic differences between Sr, Os, Li and Ca in the ocean and exogenic reservoirs allows these metals to be used as proxies for mass exchange between the surficial Earth system and the mantle, continental crust (all four) and extra-terrestrial material (Os). However, they record different geochemical pathways because they behave differently in water and have different predominant host lithologies.

Sr and Os are used as proxies for the balance between the weathering of old continental crust and juvenile basalt or direct mantle emission (e.g. Hodell et al., 1990; Goddéris and François, 1995; Tejada et al., 2009; Finlay et al., 2010; Bottini et al., 2012; Dickson et al., 2015). The fact that carbonates are the biggest source of continental Sr but not of Os (which resides predominantly in shales and evaporites), means differences in these records can be used to infer changes in weathered lithology (e.g. Peucker-Ehrenbrink et al., 1995). Li is orders of magnitude more abundant in silicates than in carbonates and thus is discussed as the most direct proxy for silicate weathering (Kısakűrek et al., 2005; Millot et al., 2010). The isotopic composition of dissolved Li is also not affected by plant growth (Lemarchand et al., 2010; Clergue et al., 2015) or phytoplankton growth (Pogge von Strandmann et al., 2016). Instead, the light Li isotope (^{6}Li) is preferentially taken up by secondary minerals (clays, oxides, zeolites) formed during weathering, enriching residual waters in isotopically heavy Li. Hence, surface water δ^7Li is controlled by the ratio of primary rock dissolution to secondary mineral formation, known as the weathering congruency (Misra and Froelich, 2012; Pogge von Strandmann and Henderson, 2015), which in turn can act as a tracer of weathering intensity (that is, the ratio of the weathering rate to the denudation rate, Dellinger et al., 2015; Pogge von Strandmann et al., 2017; Murphy et al., 2019; Gou et al., 2019). This also relates to the efficiency of CO_2 drawdown, as cations retained on the continents in secondary minerals do not end up in the oceans to assist carbon sequestration (Pogge von Strandmann and Henderson, 2015; Pogge von Strandmann et al., 2017). Ca isotopes have also been used to examine weathering processes in the geological record (Kasemann et al., 2005; Farkaš et al., 2007; Kasemann et al., 2008; Blättler et al., 2011; Holmden et al., 2012; Fantle and Tipper, 2014; Kasemann et al., 2014), but are also crucial proxies for the quantification of carbonate precipitation rates (Pogge von Strandmann et al., 2019). Because of its tight links with the marine carbonate system, Ca also serves as a constraint

https://doi.org/10.5194/gmd-2020-233
Preprint. Discussion started: 10 August 2020


Geoscientific Model Development Discussions

on CO_2 concentration. Furthermore, Ca isotopes have been considered as a potential temperature proxy (e.g. Nägler et al., 2000), but this application might be complicated by the strong control of aqueous chemistry on Ca fractionation (DePaolo, 2011). Likewise, changes in the Sr/Ca ratio in calcifiers reflects ecosystem shifts, carbonate mineralogy and calcification rate (Stoll and Schrag, 2001), and stable Sr isotopes in calcifiers correlate with growth rate, mostly influenced by temperature and pCO_2 (Stevenson et al., 2014; Müller et al., 2018). While each system individually gives valuable insight into Earth system dynamics, in concert, these trace metal systems can provide information on feedbacks and event durations, as well as improve the accuracy of our reconstructions (e.g. Kasemann et al., 2008).

3 Model implementation

We implemented the marine cycling of Sr, Os and Li and Ca isotopes in the Earth system model 'cGENIE'. cGENIE is a modular model, comprising modules for ocean physics ('GOLDSTEIN' Edwards and Marsh, 2005), marine biogeochemistry ('BIOGEM' Ridgwell et al., 2007), continental weathering and run-off ('ROKGEM' Colbourn et al., 2013), sea-floor sediment formation ('SEDGEM' Ridgwell and Hargreaves, 2007), atmospheric chemistry ('ATCHEM') and atmospheric energy balance ('EMBM' Ridgwell et al., 2007). As a whole, cGENIE includes a 3D ocean combined with a 1D atmosphere which capture the cycling of carbon and a range of other elements relevant for biogeochemical studies of the ocean water column and at the sea-sediment and sea-air interfaces, as well as climate-sensitive continental run-off and explicit sedimentary carbonate burial.

https://doi.org/10.5194/gmd-2020-233
Preprint. Discussion started: 10 August 2020

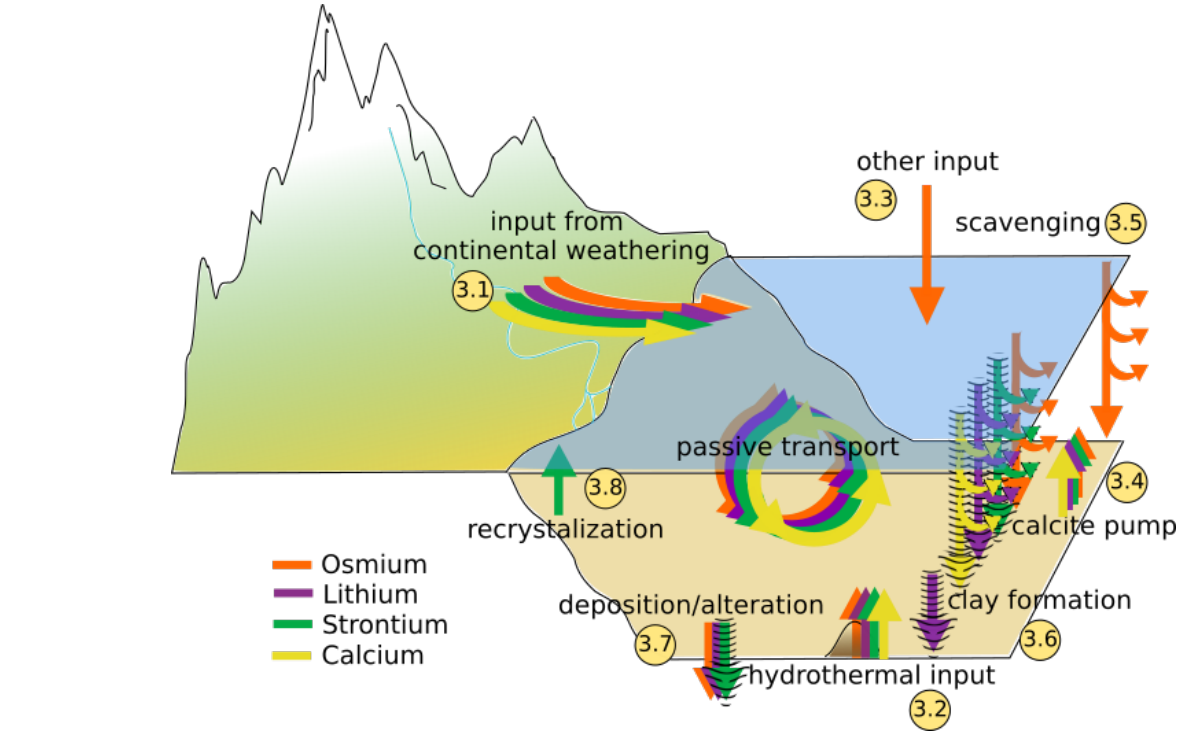

Figure 2. Processes included in the cGENIE trace metal implementation and the number of the subsection containing their explanation. Hashed arrows indicate processes during which isotopic fractionation occurs in the model.

Figure 2 shows a conceptual model of the Sr, Os, Li and Ca cycles in cGENIE with arrows of different colours showing mass fluxes of different metals. The implementation of these processes involves code additions to the modules ROKGEM, BIOGEM and SEDGEM that are described in the following sections.

3.1 Continental weathering and run-off

Continental weathering is the main source for marine Sr, Os, Li and Ca today and changes in the weathered lithology or weathering intensity are invoked as major drivers of the evolution of trace metal concentrations and their isotopic compositions in seawater over time (e.g. Misra and Froelich, 2012; Kristall et al., 2017). ROKGEM, the weathering module of cGENIE, provides a framework for calculating climate- and CO_2-dependent additions of Ca, Mg and alkalinity from carbonate weathering (following Berner, 1994) and silicate weathering (following Brady, 1991) to the ocean (see Colbourn et al., 2013, for a full description of the weathering module). The module calculates a drainage map based on a prescribed continental topography and determines the coastal locations where this input is added to the ocean. Depending on the primary source rock, we tied

https://doi.org/10.5194/gmd-2020-233
Preprint. Discussion started: 10 August 2020

Geoscientific Model Development Discussions

the rate M of Sr, Os or Li ion delivery to the ocean to Ca and magnesium (Mg) input rates from weathering of carbonates (Ca_{CaCO_3}) and/or silicates (Ca_{CaSiO_3}), related by a constant ratio k (see table 5):

$$M_{CaCO_3} = k_{CaCO_3} \cdot Ca_{CaCO_3} \qquad M_{CaSiO_3} = k_{CaSiO_3} \cdot Ca_{CaSiO_3} \tag{1}$$

ROKGEM allows for different $CaSiO_3$ weathering schemes, including one which separates the contribution from $CaSiO_3$ weathering into contributions from granite and basalt weathering ('Wallmann'). For this case, we imposed individual parameters for Sr weathering for each lithology. The model does not consider secondary mineral formation on land, which should be taken into account by setting the parameters for terrestrial Li input based on run-off data rather than source rock composition.

The amount and isotopic composition of weathering-derived Os is mostly dependent on organic matter content (Jaffe et al., 2002; Georg et al., 2013; Dubin and Peucker-Ehrenbrink, 2015). ROKGEM does not contain an explicit representation of organic matter weathering, and a differentiation between carbonate and silicate derived Os would not capture the lithology dependence of weathering derived Os appropriately. Hence, we decided not to differentiate the source lithology of Os in the model, but to prescribe the net abundance and isotopic composition of Os in continental run-off.

Table 5. Model parameters setting weathering-related trace metal fluxes.

Parameter name	default value	unit	description
`rg_par_weather_fracOs`	0.0	mol/mol	Os:[Ca+Mg] ratio in continental weathering
`rg_par_weather_CaSiO3_fracLi`	10.00E-6	mol/mol	Li:[Ca+Mg] ratio in continental silicate weathering
`rg_par_weather_CaSiO3_fracSr`	0.00532	mol/mol	Sr:[Ca+Mg] ratio in continental silicate weathering
`rg_par_weather_CaSiO3b_fracSr`	0.0057471	mol/mol	Sr:[Ca+Mg] ratio in continental basalt weathering
`rg_par_weather_CaSiO3g_fracSr`	0.0050847	mol/mol	Sr:[Ca+Mg] ratio in continental granite weathering
`rg_par_weather_CaCO3_fracSr`	0.002	mol/mol	Sr:[Ca+Mg] ratio in continental carbonate weathering

3.2 Hydrothermal inputs

Mantle-derived metal input via hydrothermal vents is parameterised in the SEDGEM module. To represent the vast range of chemical conditions and reaction rates at the sediment-water interface in the ocean efficiently, three biogeochemically distinct depositional environments are represented in SEDGEM: (1) dynamic shallow seas with reef-building biota ('reef'), (2) organic rich sediments depleted in oxygen ('muds'), and (3) plankton-derived carbonate deposition in the open ocean ('deep sea'). $CaCO_3$ deposition and dissolution as well as elemental fluxes across the sediment-water interface are parameterised differently in each of these environments, using masks to distinguish the different environments. Hydrothermal inputs of elements into bottom waters occurs only in grid cells which represent 'deep sea'. We parameterised this flux such that a global total input flux can be prescribed, which is distributed equally across 'deep sea' grid cells. There is no differentiation between seafloor areas with predominant high- or low-temperature hydrothermal venting in our implementation. Hence, we suggest to prescribe total hydrothermal metal fluxes with an average isotopic composition in cGENIE to account for both temperature regimes.

https://doi.org/10.5194/gmd-2020-233
Preprint. Discussion started: 10 August 2020


Geoscientific Model Development Discussions
Open Access
EGU

Table 6. Model parameters setting hydrothermal metal input.

Parameter name	default value	unit	description
`sg_par_sed_hydroip_fOs`	0.0	mol yr^{-1}	global hydrothermal Os flux
`sg_par_sed_hydroip_fLi`	0.0	mol yr^{-1}	global hydrothermal Li flux
`sg_par_sed_hydroip_fSr`	3.1E9	mol yr^{-1}	global hydrothermal Sr flux
`sg_par_sed_hydroip_fCa`	0.0	mol yr^{-1}	global hydrothermal Ca flux

3.3 Aeolian inputs

To account for inputs at the air-sea interface (only assumed to be relevant for Os, as described in the scientific background section), we added the option to prescribe a uniform or spatially explicit field of annual input into the surface ocean (or technically anywhere into the water column). This implementation follows the same equations of flux forcings for other marine tracers (e.g. oxygen) and is calculated as part of the BIOGEM module.

3.4 Metal export in carbonates

Ca export from the surface ocean is linked to the export of particulate organic carbon (POC) by a constant CaCO3:POC ratio (rain ratio) (see Ridgwell et al., 2007, for a description of POC export simulation in cGENIE). We parameterise the incorporation of Os, Li and Sr into carbonates by scaling their export in carbonates to the Ca export. This can be done by setting either a constant Sr/Li/Os-to-Ca ratio ($r_{M/Ca}$) or a constant scaling factor α which links the local Sr/Li/Os-to-Ca ratio in seawater to the Sr/Li/Os-to-Ca ratio in the precipitate (following e.g. Tang et al., 2008):

$$export_{metal} = k \cdot export_{Ca} \tag{2}$$

$$k = r_{M/Ca} + \alpha \cdot [Metal]_{water}/[Ca]_{water} \tag{3}$$

The Sr/Li/Os-to-Ca ratio of the precipitate is then used to calculate the metal consumption during carbonate formation, as well as metal release during carbonate dissolution. To reflect the different Sr/Li/Os-to-Ca ratios in pelagic compared to reef carbonates, a separate factor can be set for reef production. Reef $CaCO_3$ immediately contributes to surface sediments, while pelagically formed $CaCO_3$ sinks through the water-column, and might be dissolved before reaching the 'deep sea' sediment-water interface as a result of local chemical equilibria. cGENIE also calculates Li export by abiotically precipitated carbonates.

https://doi.org/10.5194/gmd-2020-233
Preprint. Discussion started: 10 August 2020

Geoscientific Model Development Discussions

Table 7. Model parameters setting the Os, Li and Sr contents of calcite shells.

Parameter name	default value	unit	description
bg_par_bio_red_CaCO3_OsCO3	0.0	mol/mol	pelagic Os:Ca ratio
bg_par_bio_red_CaCO3_OsCO3_alpha	0.0	unit-less	pelagic partition coefficient between Os and Ca
bg_par_bio_red_CaCO3_LiCO3	0.0	mol/mol	pelagic Li:Ca ratio
bg_par_bio_red_CaCO3_LiCO3_alpha	1.0	unit-less	pelagic partition coefficient between Li and Ca
sg_par_bio_red_CaCO3_LiCO3	0.0	mol/mol	benthic Li:Ca ratio
sg_par_bio_red_CaCO3_LiCO3_alpha	0.005	unit-less	benthic partition coefficient between Li and Ca
bg_par_bio_red_CaCO3_SrCO3	0.0	mol/mol	pelagic Sr:Ca ratio
bg_par_bio_red_CaCO3_SrCO3_alpha	1.0	unit-less	pelagic partition coefficient between Sr and Ca

3.5 Scavenging from the water-column

To test implications of Os burial with particulate organic carbon, we included an option for $[O_2]$-sensitive scavenging from the water column. In the surface ocean, organic carbon is produced as a function of the concentration of inorganic carbon, light, nutrient availability (PO_4^{3-} in our set up), sea ice cover and temperature (Ridgwell, 2001). The produced organic carbon is split into dissolved and particulate organic carbon (DOC and POC) at an adjustable ratio. DOC is advected and diffused in the ocean and remineralized depending on a prescribed lifetime, while POC is instantly exported to deeper water layers and remineralized following a decay function tuned to POC flux measurements (Ridgwell, 2001). O_2 is exchanged between the atmosphere and the ocean at the air-water interface, depending on the solubility of O_2 in water. In the ocean, O_2 is released during primary production in the surface ocean and consumed during remineralization of DOC and POC under oxic conditions. Following the example of existing scavenging parameterization schemes in cGENIE, we implemented this process by scaling the flux of scavenged Os (f_{scav}) to the local concentrations of Os and POC:

$$f_{scav} = k \cdot [Os] \cdot [POC] \tag{4}$$

Since there is evidence that Os needs to be reduced in order to be burried, we include a switch to use the scavenging code only where $[O_2]$ is below an adjustable threshold.

Table 8. Model parameters setting Os scavenging.

Parameter name	default value	unit	description
bg_ctrl_Os_scav_O2_dep	.false.	N/A	switch to turn on oxygen-dependent scavenging
bg_par_scav_Os_O2_threshold	5E-9	mol kg^{-1}	$[O_2]$ threshold for oxygen-dependent scavenging
bg_par_bio_remin_kOstoPOMOS	0.0	1 mol^{-1}	scaling factor for Os scavenging

https://doi.org/10.5194/gmd-2020-233
Preprint. Discussion started: 10 August 2020

Geoscientific Model Development Discussions

3.6 Clay formation

The model calculates Li burial during clay formation fLi_{clay} locally at the sea-sediment interface, which is scaled to the concentrations of Li in the deepest grid box of the water column and the detrital flux into the sediments:

$$fLi_{clay} = k \cdot [det] \cdot [Li] \tag{5}$$

Table 9. Model parameters for weathering-related trace metal fluxes.

Parameter name	default value	unit	description
`sg_par_sed_clay_fLi_alpha`	0.0	kg/mol	scaling factor relating Li burial to detrital flux and [Li]

3.7 Recrystallization

Recrystallization of $SrCO_3$ is an additional source of Sr to the water column (see above). Its parameterisation is similar to that of hydrothermal inputs, except that elemental fluxes from recrystallization only occur in bottom waters of grid cells labelled as 'reef'. The size and rate of this Sr flux can be either set as a total global or an area-weighted value.

Table 10. Model parameters for Sr recrystallization.

Parameter name	default value	unit	description
`sg_par_sed_SrCO3recrystTOT`	0.0	mol yr^{-1}	Prescribed global SrCO3 recrystlization rate
`sg_par_sed_SrCO3recryst`	0.0	mol cm^{-2} yr^{-1}	Prescribed SrCO3 recrystlization rate

3.8 Rock alteration and metal deposition at the sea floor

We include the burial of Sr and Li into seafloor sediments due to seafloor weathering by scaling the metal flux into the uppermost sediment layer ($fMetal$) to the metal concentration of the overlying ocean gridbox ($[Metal]$):

$$fMetal = k \cdot [Metal] \tag{6}$$

This burial occurs in all grid cells that are labelled as 'deep sea'. In the absence of better constraints on depositional mechanisms, we include a mathematically similar sink for Os. For a desired global burial rate B (mol s^{-1}), the value of k can be estimated by considering the total area of 'deep sea' A_{deep} (m^2) and equilibrium metal concentration $[Metal]$ (mol kg^{-1}):

$$k = \frac{B/A_{deep}}{[Metal]} \tag{7}$$

https://doi.org/10.5194/gmd-2020-233
Preprint. Discussion started: 10 August 2020


Geoscientific Model Development Discussions
Open Access
EGU

Table 11. Model parameters for metal deposition in sediments.

Parameter name	default value	unit	description
`sg_par_sed_lowTalt_fLi_alpha`	0.0	kg m^{-2} s^{-1}	Li low temperature alteration sink rate
`sg_par_sed_lowTalt_fSr_alpha`	0.0	kg m^{-2} s^{-1}	Sr low-T alteration sink rate
`sg_par_sed_Os_dep`	0.0	kg m^{-2} s^{-1}	burial rate for Os

3.9 Isotopes

The isotopic composition of Sr, Os, Li and Ca sources to the ocean is prescribed, in delta notation for stable isotopes and ratios for radiogenic isotopes. Once in the ocean, cGENIE tracks isotopes in total molar abundances rather than delta notation or ratios so that they can be advected and diffused like any other tracer. For this approach, prescribed isotopic compositions of marine inputs are converted into molar isotope abundances which requires a standard for each isotope. The hard-coded standards are listed in table 12, and are either international standards or observations of modern-day sea water. Li isotopes are implemented similarly to stable C isotopes (Ridgwell, 2001). Sr, Os and Ca are different, because they have more than two principal stable isotopes. We chose to reduce the number of traced isotopes to three for Sr and Os and two for Ca, because these subsets contain the most abundant isotopes of the respective element (Sr) and/or are most relevant for their application as seawater proxies (Sr, Os and Ca). Calcium isotopes are thus treated similarly to Li isotopes. To track three isotopes rather than two, we track two isotopes explicitly and one implicitly with the bulk abundance of the trace metal. In the case of Sr, abundances of ^{87}Sr and ^{88}Sr are tracked explicitly. The abundance of ^{86}Sr is then taken as the difference between the abundances of the two explicitly tracked isotopes and the bulk Sr abundance, since ^{84}Sr can be neglected. Os has more than two stable isotopes, but only two of them, ^{187}Os and ^{188}Os, are currently used as a proxy system and so these two isotopes are tracked explicitly and the bulk Os abundance contains all remaining stable isotopes. To account for isotopic fractionation during chemical reactions, the amount fI of an isotope I transferred to the product-side of the reaction is calculated by multiplying the amount of Sr, Li or Ca involved in the reaction, fM, with the relative abundance k of I in the reaction product:

$$fI = k \cdot fM \tag{8}$$

k is derived from the prescribed relative abundance of I in the reaction product in standard sea water, usually the observed isotopic signature of the respective reaction product in today's ocean, and the difference between the local, simulated relative abundance of I in cGENIE and standard sea water.

The model parameters required to set isotopic fractionation of Os, Li and Sr are listed in table 13. Given the current lack of evidence for Os isotopic fractionation outside of the lithosphere (e.g. Nanne et al., 2017) we do not include a fractionation factor for marine Os sinks. For Sr and Li, we include isotopic fractionation during carbonate and secondary mineral formation. We simplify the model by assuming constant fractionation factors as the influence of environmental factors on isotope partitioning

https://doi.org/10.5194/gmd-2020-233
Preprint. Discussion started: 10 August 2020

Geoscientific Model Development Discussions
Open Access
EGU

is still debated. Growth rate-dependent fractionation factors could be implemented in the future by using the ecosystem module ECOGEM (Ward et al., 2018), but this will significantly increase computational costs.

Table 12. Isotopic standards in cGENIE.

Isotope ratio	standard value	standard material/reference
$^{87}Sr/^{86}Sr$	0.709175	Mokadem et al. (2015)
$^{88}Sr/^{86}Sr$	8.375209	NBS987
$^{187}Os/^{188}Os$	1.05	Lu et al. (2017)
$^{188}Os/^{189+190+192}Os$	0.159	Dąbek and Halas (2007)
$^{7}Li/^{6}Li$	12.33333	L-SVEC
$^{44}Ca/^{40}Ca$	0.021229	NIST SRM915aHeuser et al. (2002)

https://doi.org/10.5194/gmd-2020-233
Preprint. Discussion started: 10 August 2020

Geoscientific Model Development Discussions
Open Access
EGU

Table 13. Model parameters for the representation of isotopes and isotopic fractionation.

Parameter name	default value	unit	description
rg_par_weather_187Os_188Os	0.0		$^{187}Os/^{188}Os$ of input from weathering
rg_par_weather_188Os_192Os	0.0		proportional ^{188}Os abundance in input from weathering
sg_par_sed_hydroip_fOs_187Os_188Os	0.0		$^{187}Os/^{188}Os$ of hydrothermal input
sg_par_sed_hydroip_fOs_188Os_192Os	0.0		proportional ^{188}Os abundance in hydrothermal input
bg_par_d7Li_LiCO3_epsilon	4.0	‰	δ^7Li fractionation for pelagically formed carbonate
sg_par_d7Li_LiCO3_epsilon	-2.0	‰	δ^7Li fractionation for neritically formed carbonate
sg_par_sed_hydroip_fLi_d7Li	4.0	‰	δ^7Li of hydrothermal input
sg_par_sed_lowTalt_7Li_epsilon	-15.0	‰	δ^7Li of sea floor alteration sink
sg_par_sed_clay_7Li_epsilon	-15.0	‰	δ^7Li of clay
rg_par_weather_CaSiO3_Li_d7Li	0.0	‰	δ^7Li of input from silicate weathering
bg_par_d88Sr_SrCO3_epsilon	-0.236	‰	$\delta^{88/86}Sr$ fractionation for pelagically formed carbonate
sg_par_d88Sr_SrCO3_epsilon	0.9	‰	$\delta^{88/86}Sr$ fractionation for neritically formed carbonate
sg_par_r87Sr_SrCO3recryst	0.70838		$^{87}Sr/^{86}Sr$ of input from recrystalization
sg_par_d88Sr_SrCO3recryst	0.172	‰	$\delta^{88/86}Sr$ of input from recrystalization
sg_par_sed_hydroip_fSr_r87Sr	0.7025		$^{87}Sr/^{86}Sr$ of hydrothermal input
sg_par_sed_hydroip_fSr_d88Sr	0.24	‰	$\delta^{88/86}Sr$ of hydrothermal input
rg_par_weather_CaSiO3_r87Sr	0.714		$^{87}Sr/^{86}Sr$ of silicate weathering
rg_par_weather_CaSiO3b_r87Sr	0.705		$^{87}Sr/^{86}Sr$ of basaltic silicate weathering
rg_par_weather_CaSiO3g_r87Sr	0.719		$^{87}Sr/^{86}Sr$ of granitic silicate weathering
rg_par_weather_CaCO3_r87Sr	0.7077		$^{87}Sr/^{86}Sr$ of carbonate weathering
rg_par_weather_CaSiO3_d88Sr	0.36	‰	$\delta^{88/86}Sr$ of silicate weathering
rg_par_weather_CaSiO3b_d88Sr	0.36	‰	$\delta^{88/86}Sr$ of basaltic silicate weathering
rg_par_weather_CaSiO3g_d88Sr	0.36	‰	$\delta^{88/86}Sr$ of granitic silicate weathering
rg_par_weather_CaCO3_d88Sr	0.16	‰	$\delta^{88/86}Sr$ of carbonate weathering
rg_par_weather_CaCO3_d44Ca	0.8	‰	$\delta^{44}Ca$ of carbonate weathering
rg_par_weather_CaSiO3_d44Ca	0.8	‰	$\delta^{44}Ca$ of silicate weathering
sg_par_sed_hydroip_fCa_d44Ca	0.9	‰	$\delta^{44}Ca$ of hydrothermal input
sg_par_d44Ca_CaCO3_epsilon	-1.07	‰	$\delta^{44}Ca$ fractionation for neritically form carbonates
bg_par_d44Ca_CaCO3_epsilon	-1.09	‰	$\delta^{44}Ca$ fractionation for pelagically form carbonates

https://doi.org/10.5194/gmd-2020-233
Preprint. Discussion started: 10 August 2020

Geoscientific Model Development Discussions

4 Model configuration and validation

Box models are important tools to investigate the global balance of elemental and isotopic fluxes and essential to estimate elemental residence times as well as to identify missing sinks and sources (e.g. Stoffyn-Egli and Mackenzie, 1984). They are usually validated with observed average seawater compositions (e.g. Krabbenhöft et al., 2010; Misra and Froelich, 2012; Pearce et al., 2015). The three-dimensional grid of cGENIE allows for comparison of the spatial pattern produced by the simulated set of processes to observations, which can further bolster or refute the accuracy of our assumptions about global trace metal cycling on diverse time scales. Here we set up the model to represent the pre-industrial state of trace metal cycling, and compare the model output to measured modern seawater profiles.

4.1 Pre-industrial configuration

We initialised cGENIE with a modern-day geography on a 36x36 grid with up to 8 depth layers in the ocean (following Ridgwell and Hargreaves, 2007) and with a pre-industrial CO_2 concentration of 278 ppm. Marine biological productivity is simulated using a single nutrient scheme as outlined in Ridgwell et al. (2007) but with a constant $CaCO_3$:POC rain ratio set to 0.043 (Panchuk et al., 2008). Burial and dissolution of $CaCO_3$ in deep-sea sediments follows Ridgwell and Hargreaves (2007). This configuration results in a pelagic $CaCO_3$ burial rate of 0.125 GtC yr^{-1}, close to the observationally calibrated $CaCO_3$ sink of Ridgwell and Hargreaves (2007). In addition to the pelagic environment, covering 350.6 million km^2, we simulated reef deposition on shelfs, which covers 5.5 million km^2 in our set up. The sediment model bathymetry was derived from ETOPO5[1]. Reefal deposition was simulated in grid cells representing marine sediments shallower than 1000 m and not further pole-wards than 41.8° N/S, on the basis that reefal carbonate deposition is predominantly a tropical and subtropical process. We prescribe a reefal $CaCO_3$ sink of 0.04 GtC yr^{-1}. Temperature dependent terrestrial silicate and carbonate weathering (Lord et al., 2016) were included with the baseline temperature and rates of $CaCO_3$ and $CaSiO_3$ weathering set to 8.48°C, 8.4 Gmol yr^{-1} and 6.0 Gmol yr^{-1}, respectively. Silicate weathering was split into weathering of $CaSiO_3$ (2/3) and $MgSiO_3$ (1/3). We balanced the Ca cycle by including an exchange between sedimentary Ca and dissolved Mg of 2.0 Gmol yr^{-1} at the seafloor. To close the long-term carbon cycle, we prescribed a fixed rate of organic C burial of 2.57 Gmol yr^{-1} with $\delta^{13}C$ = -30 ‰ as well as a total exogenic carbon flux of 8.57 PgC yr^{-1} with $\delta^{13}C$ = -6 ‰. This net input can be regarded as the result of 8.57 PgC yr^{-1} sub-aerial outgassing with $\delta^{13}C$ = -4.6 ‰ (Mason et al., 2017), hydrothermal emissions of 1.5 PgC yr^{-1} with $\delta^{13}C$ = -6 ‰ at mid-ocean ridges and consumption of 1.5 PgC yr^{-1} with $\delta^{13}C$ = 2 ‰ during seafloor weathering (Cocker et al., 1982). Table 14 summarizes the trace metal fluxes we prescribe to simulate the pre-industrial trace metal cycling. Note that the prescribed hydrothermal metal fluxes are net fluxes of high- and low-temperature hydrothermal activity.

By applying the chosen model parameters for our spin-up with modern boundary conditions and running the model to steady state, we assumed that metal fluxes are currently in equilibrium. This is a common assumption when modelling weathering tracer isotopes and their perturbations in the geologic record (e.g. Misra and Froelich, 2012; Bauer et al., 2017). However, given the long residence time estimates in today's ocean, it is likely that at least the Sr, Li and Ca cycles are not fully in steady state

[1]Data Announcement 88-MGG-02, Digital relief of the Surface of the Earth. NOAA, National Geophysical Data Center, Boulder, Colorado, 1988.

https://doi.org/10.5194/gmd-2020-233
Preprint. Discussion started: 10 August 2020


Geoscientific Model Development Discussions

today (i.e. Derry, 2009). Constant Os isotopic compositions of seawater over the last millennia suggest that Os has reached steady state since the last deglaciation, but residence time estimates of >20 kyr based on modern day Os fluxes put this into question (Oxburgh, 2001). The newly implemented tracers in cGENIE can be used to study different equilibria and transient adaptations of the marine metal reservoirs to new boundary conditions. As an example, we simulated two different steady states for Sr under pre-industrial boundary conditions: One with a best estimate of pre-industrial Sr fluxes (hereafter referred to as FLUXES) and one tuned to best fit the spatial mean of observations (TUNED).

https://doi.org/10.5194/gmd-2020-233
Preprint. Discussion started: 10 August 2020

Geoscientific Model Development Discussions

Table 14. Metal fluxes for pre-industrial spin up.

Flux		size (mol yr^{-1})	isotopic composition	
Strontium				
			$^{87}Sr/^{86}Sr$	$\delta^{88/86}Sr$ (‰)
weathering	FLUXES	34.0x10^9	0.7122	0.318
	TUNED	31.0x10^9	0.7097	0.256
hydrothermal input		3.1x10^9	0.7038	0.261
diagenetic input	FLUXES	3.4x10^9	0.708	0.385
	TUNED	3.4x10^9	0.7087	0.256
carbonate sink	FLUXES	40.5x10^9	seawater	seawater - 0.18
	TUNED	37.5x10^9	seawater	seawater - 0.18
Osmium				
			$^{187}Os/^{188}Os$	$^{188}Os/^{189+190+192}Os$
weathering		2605.26	1.2	0.159
hydrothermal input		526.32	0.5625	0.159
aeolian input		157.89	0.2	0.159
sediment deposition		3289.47	seawater	seawater
carbonate sink		0.0	seawater	seawater
Lithium				
			δ^7Li (‰)	
weathering		8x10^9	23.0	
hydrothermal input		6x10^9	8.3	
secondary mineral formation sink		4x10^9	seawater -15.0	
sea floor alteration sink		9.5x10^9	seawater -15.0	
carbonate sink		0.5x10^9	seawater - 4	
Calcium				
			$\delta^{44}Ca$ (‰)	
weathering		12.4x10^{12}	0.9	
hydrothermal input		2x10^{12}	0.93	
carbonate sink		14.4x10^{12}	seawater - 1.1	

The spin up was done in three stages to improve computational efficiency. The first stage (20 kyr) was run with a closed marine carbonate system, where the marine C and alkalinity reservoirs are artificially restored by balancing losses through $CaCO_3$ burial with external inputs to the ocean. During this stage, the climate and ocean dynamics adjust to the physical

https://doi.org/10.5194/gmd-2020-233
Preprint. Discussion started: 10 August 2020

boundary conditions and ocean-atmosphere C exchanges balance. In the second phase (500 kyr) the marine carbonate system was open so that prescribed inputs from terrestrial weathering and the mantle and marine burial dynamically adjusted to balance. During the third stage (15 Myr), when ocean dynamics, C, nutrient and Ca cycles were already equilibrated, the prescribed Sr, Os and Li sources were added and the model was run until metal concentrations and their isotopic composition in the ocean were at steady state. The model calculations were accelerated during the last two stages of the spin up using the time-stepping method introduced by Lord et al. (2016).

4.2 Comparison between simulated and observed trace metal contents of seawater

One advantage of simulating trace metal cycles within a 3D earth system model is that we can test, for the first time, simulated metal concentrations and isotopes against observed spatial patterns. In the following sections, the simulated pre-industrial distribution of each metal is compared against observational data shown in section 2.5.

https://doi.org/10.5194/gmd-2020-233
Preprint. Discussion started: 10 August 2020

Geoscientific Model Development Discussions

4.2.1 Strontium

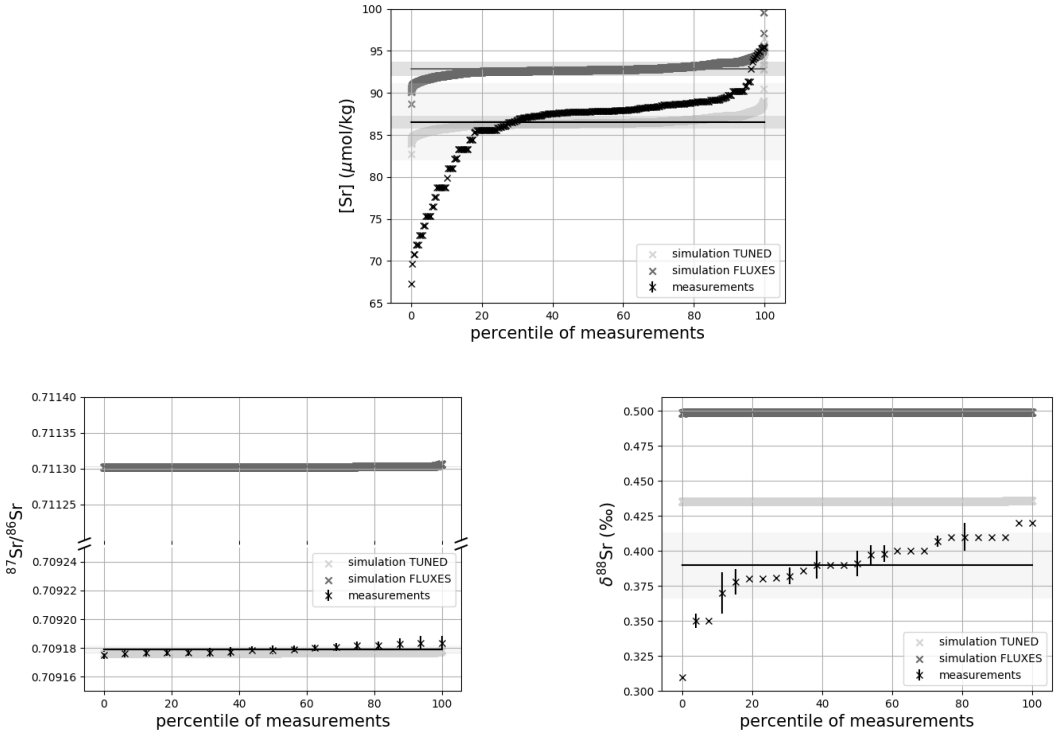

Figure 3. Comparison between measured and simulated Sr composition of seawater. Shown are measured Sr concentrations and isotope ratios and the values of all ocean grid cells from the model simulations, sorted by value from smallest to biggest. Mean concentrations and isotope ratios are indicated by horizontal lines, and shading indicates one standard deviation around the means. Data is taken from Angino et al. (1966), Fabricand et al. (1967), Bernat et al. (1972), Brass and Turekian (1974), De Villiers (1999), Mokadem et al. (2015) and Wakaki et al. (2017).

Figure 3 compares Sr concentrations and isotopic compositions in our simulation with observations. Standard deviations tend to be smaller in the model simulations than in observations. This is particularly true for Sr concentrations which are more homogeneous in the simulations than in observations. Measured isotopic compositions of Sr in seawater are very homogeneous, which is matched by the model simulations. The FLUXES simulation, in which we constrain fluxes rather than the marine reservoir with observations, results in higher than observed Sr concentrations in seawater, and a more radiogenic and isotopically heavy composition. Uncertainties in size and isotopic composition of pre-industrial Sr fluxes are big enough to allow for realistic combinations that lead to equilibrated Sr concentrations close to observations (TUNED simulation) but continental input needs to be less radiogenic than the average of today's rivers to yield a steady state marine $^{87}Sr/^{86}Sr$ close to obser-

https://doi.org/10.5194/gmd-2020-233
Preprint. Discussion started: 10 August 2020

Geoscientific Model Development Discussions

vations (in agreement with e.g. Pearce et al., 2015). The observed fractionation factor for stable Sr isotopes during biogenic $CaCO_3$ formation is too big to equilibrate the model at the observed low δ^{88}Sr, even if we assume that all Sr sources only provide mantle-like light Sr (δ^{88}Sr = 0.256‰, TUNED simulation). Corroborating the conclusion of e.g. Vance et al. (2009), this suggests that the isotopic composition of marine dissolved Sr is currently not at equilibrium.

The simulations capture the homogeneous distribution of Sr concentrations observed at most site (see figures A1 and A2 in the SI). However modelled Sr concentrations are higher than observed in some studies of North Atlantic water. Given that the low North Atlantic values come from one of the first studies measuring Sr concentrations in seawater (Angino et al., 1966), and that other studies of North Atlantic seawater yielded higher Sr concentrations (e.g. De Villiers, 1999), this difference could be partially the result of analytical errors or seasonal/inter-annual variability.

4.2.2 Osmium

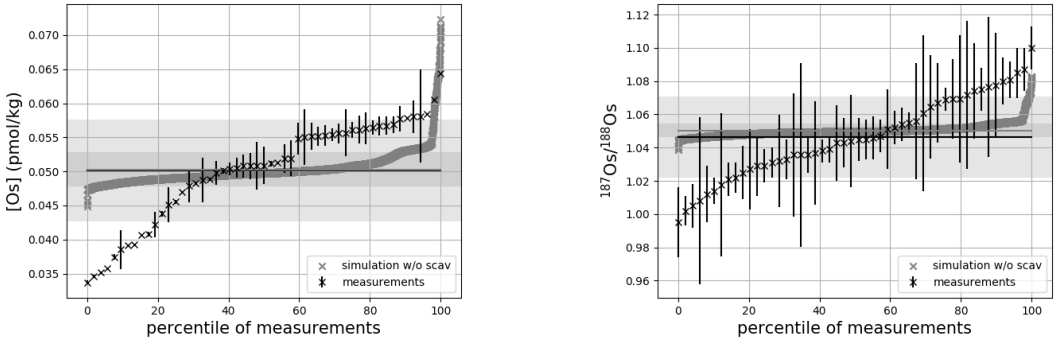

Figure 4. Comparison between measured and simulated Os composition of seawater. Shown are all available measured Os concentrations and isotope ratios and the values of all ocean grid cells in the simulation, sorted by value from smallest to biggest. Mean concentrations and isotope ratios are indicated by horizontal lines, and shading indicates one standard deviation around the means. Data is taken from Levasseur et al. (1998), Woodhouse et al. (1999) and Gannoun and Burton (2014).

Os concentrations and isotopes are generally more homogeneous in the simulation than in the observations. While the model captures the range of 80% of the measured Os concentrations and isotopic compositions well, it fails to reproduce the lowest 20% of measurements, especially with respect to Os concentrations. The low Os concentrations not captured by the model are observations from surface and intermediate waters from the East Pacific (fig. A3, Woodhouse et al., 1999; Gannoun and Burton, 2014). Since the depletion of Os in Pacific surface waters is a robust feature against measurement methods, this indicates that some processes affecting Os distribution in that region might be missing in our model. For example, Woodhouse et al. (1999) suggested that Os could bind onto organic matter in the water column under low oxygen conditions. cGENIE provides the necessary framework to investigate this and other assumptions, which should be the subject of a separate study. Our aim here is to focus on reproducing the basin-scale distribution in trace metals. Observations from other sites show no vertical Os

https://doi.org/10.5194/gmd-2020-233
Preprint. Discussion started: 10 August 2020

Geoscientific Model Development Discussions

concentration gradients, which is well-reproduced by our simulation set-up. The isotopic Os composition shows a uniform vertical distribution in the simulations, which is consistent with observations at all sites (see figures A3b).

4.2.3 Lithium

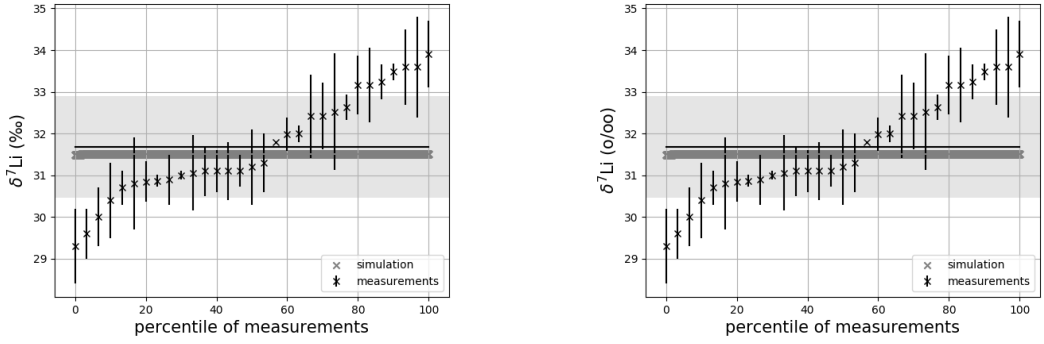

Figure 5. Comparison between measured and simulated Li composition of seawater. Shown are all available measured Li concentrations and isotope ratios and the values of all ocean grid cells in the simulation, sorted by value from smallest to biggest. Mean concentrations and isotope ratios are indicated by horizontal lines, and shading indicates one standard deviation around the means. Data is taken from Angino and Billings (1966), Fabricand et al. (1967), Chan (1987), Chan and Edmond (1988), You and Chan (1996), Moriguti and Nakamura (1998), Tomascak et al. (1999), James and Palmer (2000), Košler et al. (2001), Nishio and Nakai (2002), Hall, Bryant et al. (2003), Pistiner and Henderson (2003), Millot et al. (2004), Choi et al. (2010), Pogge von Strandmann et al. (2010), Phan et al. (2016), Lin et al. (2016), Henchiri et al. (2016), Weynell et al. (2017), Fries et al. (2019), Gou et al. (2019), Hindshaw et al. (2019), Murphy et al. (2019) and Pogge von Strandmann et al. (2019).

Similar to Sr and Os, the model simulates more homogeneous Li concentrations and isotopic compositions than is observed for most of the ocean (see fig. 5). The simulated standard deviation around the spatial mean of Li concentrations is only 8% of that observed. The lowest and highest 20% of observed Li concentrations is not reproduced by our simulation set-up. Similarly, there are no spatial gradients in the simulated isotopic composition of dissolved Li, while observations show some spread. Given relatively large analytical uncertainty, it is more likely that this results from measurement inconsistencies rather than unknown processes affecting the isotopic composition of dissolved Li.

The high concentrations which are underrepresented in our simulation were mostly measured in the upper water column (see fig. A4). As shown in fig. A1, these measurements all come from one study in the Caribbean Sea (Angino and Billings, 1966), a marginal ocean which is not representative of the open ocean and which can barely be resolved in the coarse grid of cGENIE. Additionally, Angino and Billings (1966) was one of the first studies measuring Li concentrations in seawater, and their measurements may be associated with much larger uncertainties than reported. Were these measurements excluded, the spatial mean of observed Li concentrations would be lower, and the model could be re-tuned by prescribing slightly lower Li fluxes in- and out of the ocean which are permissible given the current range of flux estimates (see table 3).

https://doi.org/10.5194/gmd-2020-233
Preprint. Discussion started: 10 August 2020

Geoscientific Model Development Discussions

Only one measured vertical profile of Li isotopes is available in the literature (Hall), and it shows no vertical δ^7Li variation which is reproduced by our simulation. The simulated ^{7}Li is offset from the profile reported by Hall since we tuned the model to the average of reported seawater ^{7}Li measurements but the profile in Hall contains some of the most ^{7}Li enriched published seawater values.

4.2.4 Calcium

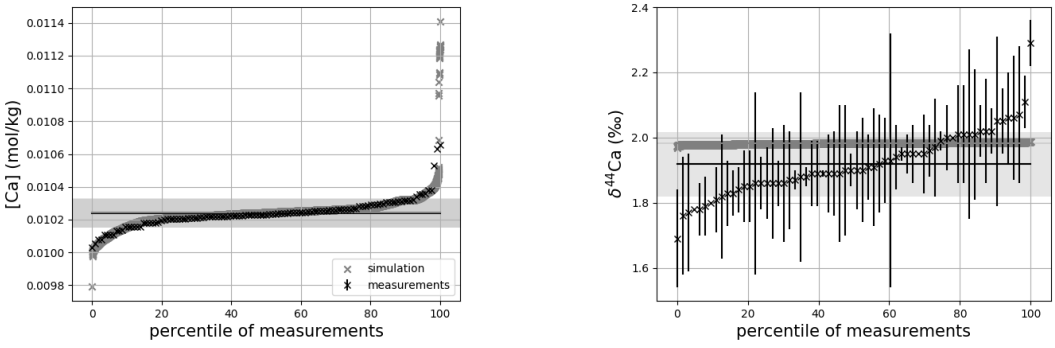

Figure 6. Comparison between measured and simulated Ca composition of seawater. Shown are all available measured Ca concentrations and isotope ratios and the values of all ocean grid cells in the simulation, sorted by value from smallest to biggest. Mean concentrations and isotope ratios are indicated by horizontal lines, and shading indicates one standard deviation around the means. Data is taken from Fabricand et al. (1967), De Villiers (1999) and Fantle and Tipper (2014).

Simulated concentrations of dissolved Ca and its homogeneous isotopic composition closely resemble the observations. Similar to the average Ca concentration in seawater, the uniform vertical distribution is well captured by the model simulation (see fig. A5). Likewise, no vertical Sr/Ca gradients are observed or simulated. Observed Sr/Ca ratios are in between simulation results with tuned and un-tuned marine Sr reservoir. This is an artefact of the tuning to mean observed Sr concentrations which is lower than the mean Sr concentrations of the sites shown in figure A5 because it includes the unusually depleted samples from the North Atlantic. This mismatch is another indication that the Sr measurements reported in Angino et al. (1966) might be associated with a larger uncertainty than reported.

4.3 Transient perturbation experiments

Another advantage of the new metal cycles in cGENIE is that we can study their transient behaviour under external forcings in a fully coupled system, including effects from ocean circulation and primary productivity changes, climate-sensitive weathering and marine carbonate accumulation and dissolution. Here we present one example, where we instantly release either 1000 Pg C or 5000 Pg C into the atmosphere to produce temporary weathering responses which re-equilibrate the model (similar to Lord et al., 2016). These scenarios allow us to showcase the sensitivity of the simulated metal systems and to discuss the Earth system processes that shape their transient evolution. Since our experiment are set up to understand model behaviour,

https://doi.org/10.5194/gmd-2020-233
Preprint. Discussion started: 10 August 2020

Geoscientific Model Development Discussions
Open Access
EGU

it is of less concern here whether these scenarios cause isotopic perturbations beyond the analytical uncertainty of real-world measurements.

Table 15. Marine trace metal concentrations and residence times in our pre-industrial spin up compared to those reported in literature (see scientific background).

Metal	mean concentration (mol kg^{-1})	simulated residence time (yr)	estimated residence time (yr)
Strontium FLUXES	92.84×10^{-6}	~2,100,000	1,900,000–3,450,000
Strontium TUNED	86.50×10^{-6}	~1,960,000	1,900,000–3,450,000
Osmium	52.64×10^{-15}	~21,500	3,000–50,000
Lithium	27.00×10^{-6}	~2,600,000	300,000–3,000,000
Calcium	10.25×10^{-3}	~960,000	500,000–1,300,000

In our spin-up, the prescribed metal fluxes result in residence times within the range of published estimates (table 15). Li has the longest residence time in our simulations, and thus the largest inertia to external perturbations. Sr and Ca follow, with Os being the most responsive system.

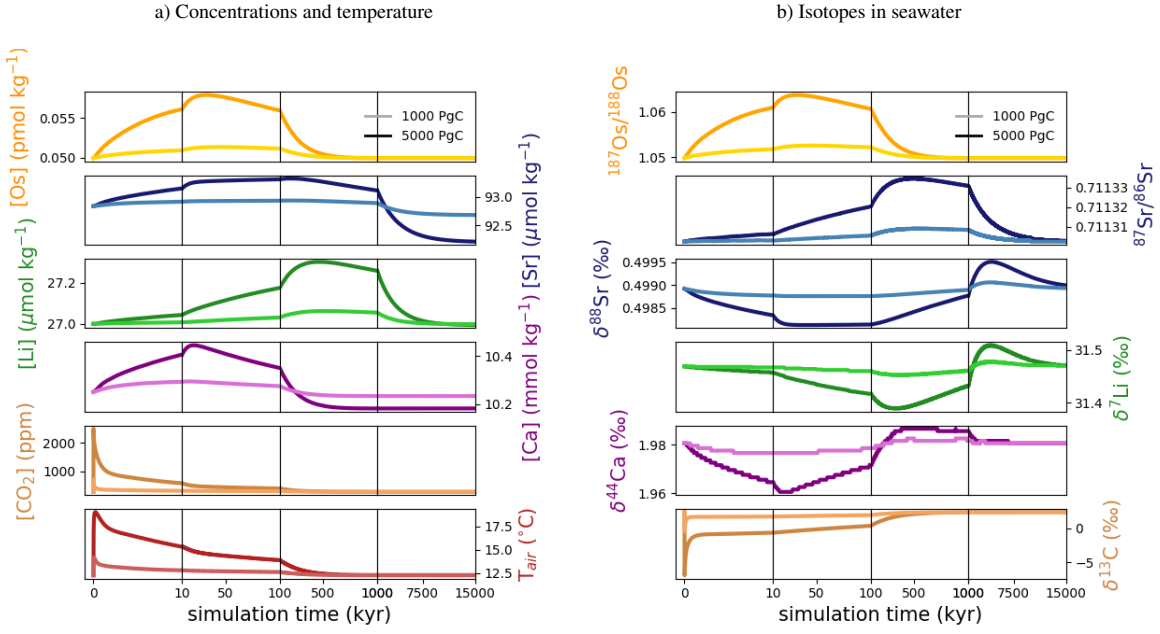

Figure 7. Transient changes in modelled Sr, Os, Li, Ca, composition of seawater and atmospheric CO_2 and temperature following instant releases of 1000 Pg C and 5000 Pg C. Shown are changes a) in concentrations, and b) in isotopic composition of seawater.

https://doi.org/10.5194/gmd-2020-233
Preprint. Discussion started: 10 August 2020


Geoscientific Model Development Discussions

Fig. 7 shows the modelled transient responses of Sr, Os, Li, Ca concentrations and isotopic compositions, DIC δ^{13}C, atmospheric CO_2 and temperature to an exogenic CO_2 pulse. After the instantaneous carbon release, atmospheric CO_2 concentration increases and the δ^{13}C of seawater decreases on the timescale of years. The sudden increase in atmospheric CO_2 concentrations replenishes the marine carbon reservoir, which decreases biogenic carbonate formation in the surface ocean and leads to the dissolution of pelagic carbonates. Over the next ~10,000 yrs, this negative carbon cycle feedback removes the majority of the initial excess carbon (Lord et al., 2016). Increased atmospheric CO_2 also enhances the greenhouse effect and thus leads to a rise in global mean air temperature, altering the hydrological cycle and speeding up reaction rates which result in increased rates of continental crust weathering. After a few ten thousands of years, increased continental weathering supplies enough alkalinity to the ocean to slow down carbonate dissolution and increase carbonate burial. Through enhanced silicate weathering and carbonate burial, the remaining excess carbon is sequestered over the timescale of ~100,000 yrs after the emission. Over the same timescale, temperature, which due to Earth system feedbacks initially recovers more slowly than atmospheric CO_2 concentrations, returns to pre-emissions values and ends the phase of enhanced weathering. Metal input from continental weathering (and marine carbonate dissolution for Sr and Ca) leads to a transient growth of marine metal reservoirs and isotopic excursions. Increased continental weathering increases the influx of radiogenic Sr and Os, driving the respective marine reservoirs to more radiogenic isotopic compositions. Continental crust is also depleted in heavy stable isotopes compared to seawater, and the increased weathering influx therefore reduces the δ^{88}Sr, δ^{7}Li and δ^{44}Ca values of seawater. The isotopic composition of carbonates and silicates in continental crust is fixed in our set-up, but since carbonate and silicate weathering rates vary differently with climate, the isotopic composition of weathering-derived marine input varies for metals with different isotopic compositions in these lithologies. For example, the radiogenic Sr excursion in the ocean is amplified by a transient increase in $^{87}Sr/^{86}Sr$ of weathering-derived Sr. Since more alkalinity than Ca^{2+} is derived from continental weathering in our set-up, the climate-driven increase in weathering results in a transient imbalance between alkalinity and Ca^{2+} supplies which does not appear in C cycle simulations without an igneous Ca^{2+} source at the seafloor (e.g. Lord et al., 2016; Vervoort et al., 2019). The imbalance is small (10% of the Ca input at its peak) but cumulatively the unbalanced alkalinity supply is large enough to causes a slight reduction of the steady-state marine Ca and Sr reservoirs (by ~0.5% following the emission of 5000 Pg C). Our assumption of a climate-insensitive Ca^{2+} source at the seafloor is a simplification since there is evidence that this flux depends on bottom water properties, in particular temperature (e.g. Krissansen-Totton and Catling, 2017). However, the climate sensitivity of this Ca^{2+} flux is lower than that from continental weathering (Brady and Gíslason, 1997) and temperature change is dampened in the deep ocean. In our transient simulations this would mean that Ca^{2+} supply from the seafloor would increase less than from the continent, were this climate sensitivity to be included in the model. Without this additional feedback, our set-up thus produces an upper limit for a transient imbalance between alkalinity and Ca^{2+} supplies which is the consequence of decoupled alkalinity and Ca^{2+} sources with different climate sensitivities.

In the presented simulations, only the radiogenic $^{87}Sr/^{86}Sr$ excursion amplitude is larger than measurement uncertainty in present-day seawater (see figures 3 – 6). Stronger or prolonged climate change, or a more sensitive weathering regime, would be required to produce detectable weathering changes in the other isotope systems. However, our simulation results still illustrate the different responses of all five isotope systems to a sudden carbon injection. The timings of excursion peaks and minima

https://doi.org/10.5194/gmd-2020-233
Preprint. Discussion started: 10 August 2020


Geoscientific Model Development Discussions

differ strongly between the isotope systems. The radiogenic $^{187}Os/^{188}Os$ and negative $\delta^{88}Sr$ and $\delta^{44}Ca$ excursions peak a few tens of thousands of years after the C injection, while the radiogenic $^{87}Sr/^{86}Sr$ and negative $\delta^{7}Li$ excursions take hundreds of thousands of years to reach their full amplitude. These time lags result from different residence times and fractionation processes:

With the shortest residence time, estimated both from present-day inventories and in our simulation (see table 15), Os is the first metal to re-equilibrate after the perturbation. The excursions in Os concentration and isotopes are only driven by enhanced weathering rates, and thus both recover within 300 kyrs once atmospheric temperature, and with it continental weathering rates, decrease sufficiently. The radiogenic $^{87}Sr/^{86}Sr$ excursion, however, continues to grow until weathering rates have fully returned to pre-event levels because concentration-dependent Sr sinks adapt more slowly to enhanced continental Sr input as a result of the longer residence time. The re-equilibration of the marine Sr reservoir is substantially slower than that of the Os reservoir for the same reason. However, the removal of marine Sr is also dependent on carbonate chemistry, since marine carbonate preservation constitutes the largest marine Sr sink. Biogenic carbonate preservation initially decreases because of the pH drop following the C injection, but it increases during the C cycle recovery as a result of enhanced weathering-related alkalinity input. The increased marine carbonate burial causes the marine Ca reservoir to re-equilibrate on a similar timescale to Os although Ca has a substantially longer residence time in our spin-up. The effect is not strong enough to stop the growth of the marine Sr reservoir but it reduces its growth rate. Isotopic fractionation of Ca and Sr during biogenic carbonate formation enhances the speed of the $\delta^{44}Ca$ recovery and stops the $\delta^{88}Sr$ excursion from growing, despite continued excess input of isotopically light continental Sr. Li has the longest residence time of the four metals in our simulations and Li burial is only dependent on the marine Li concentration and a constant detrital flux, not carbonate chemistry. Hence, the marine Li reservoir continues to grow until all excess weathering stops. Once more dissolved Li is buried than added to the ocean, i.e. the marine Li reservoir shrinks, the $\delta^{7}Li$ trend is reverses because excess sources of isotopically light Li cease and isotopically light Li is preferentially buried during clay formation, enriching seawater in the heavier ^{7}Li. In the longer term, stable isotope fractionation during the removal of excess Sr, Li and Ca from the ocean results in transient positive $\delta^{88}Sr$, $\delta^{7}Li$ and $\delta^{44}Ca$ excursions which, in the case of Sr and Li, last for several million years. In our simulations, the staggered timings of the $^{187}Os/^{188}Os$ and $^{87}Sr/^{86}Sr$ excursion peaks, as well as the $\delta^{44}Ca$ and $\delta^{7}Li$ excursion minima, are thus predominantly the result of different elemental residence times while enhanced carbonate burial is the main reason for the time lag between $\delta^{7}Li$ and $\delta^{88}Sr$ and the coincidence of the excursion minima of $\delta^{88}Sr$ and $\delta^{44}Ca$.

5 Conclusions

Sr, Os, Li and Ca isotope records can help identify mantle activity and lithological responses to climate change in the geological record if processes governing their distribution in the ocean and their response to geological perturbations were well understood. Our implementation of the marine cycling of Sr, Os, Li and Ca in the Earth system model cGENIE allows us to investigate these processes and their consistency with observations. Simulating pre-industrial Sr, Os, Li and Ca distributions in the ocean, the model achieves slightly more homogeneous fields than observed, but consistent with the widely used assumption

https://doi.org/10.5194/gmd-2020-233
Preprint. Discussion started: 10 August 2020

of homogeneous metal isotope distributions in a fully equilibrated state (e.g. Elderfield, 1986; Chan and Edmond, 1988). It reproduces the mostly homogeneous mean observed depth profiles of concentrations and isotopic compositions well, but partially deviates from local observations. This could be an artefact of measurement uncertainties, non-equilibrated cycles in today's ocean or local processes not resolved or parameterised in cGENIE. We showed how the new cGENIE tracers thus provide an opportunity to investigate the consistency between reported metal compositions in the ocean and marine sources and sinks, and between different ocean basins. Further investigations of the differences between cGENIE simulations and observations have thus the potential to improve our understanding of present-day marine trace metal cycling. Furthermore, the new implementation can be used to study the response of these metal cycles to transient environmental change. As an example, we show how these systems react to a sudden CO_2 release through perturbation to their input and output fluxes on different timescales. cGENIE thus becomes a valuable tool to improve our understanding of Sr, Os, Li and Ca isotopes and distributions in today's ocean, and to quantitatively interrogate the environmental signals of these isotope systems as preserved in sedimentary records.

Code availability. The model source code, as well as the simulation configuration files, are publicly available and can be accessed on github. The repository https://github.com/derpycode/cgenie.muffin contains the model source code, which comes with a MIT license (©Andy Ridgwell 2020). The present manuscript refers to the cgenie.muffin release v.0.9.10, which is archived on Zenodo (DOI 10.5281/zenodo.3620846). A detailed documentation of the model download, installation, execution and visualization of results, as well as a range of example configurations, is available from:

http://www.seao2.info/cgenie/docs/muffin.pdf

Configuration files for the specific experiments presented in this manuscript are provided in the folder GMD_adloffetal.2020, which can be obtained from:

https://github.com/markusadloff/Publication_resources

Details of each simulation plus the command lines needed to perform them, are given in readme.txt. The repository version relevant for this manuscript is v1.0, which is also archived on Zenodo (DOI: 10.5281/zenodo.3972011)

https://doi.org/10.5194/gmd-2020-233
Preprint. Discussion started: 10 August 2020

Geoscientific Model Development Discussions
Open Access
EGU

Appendix A: Observed and simulated metal distributions in the water column

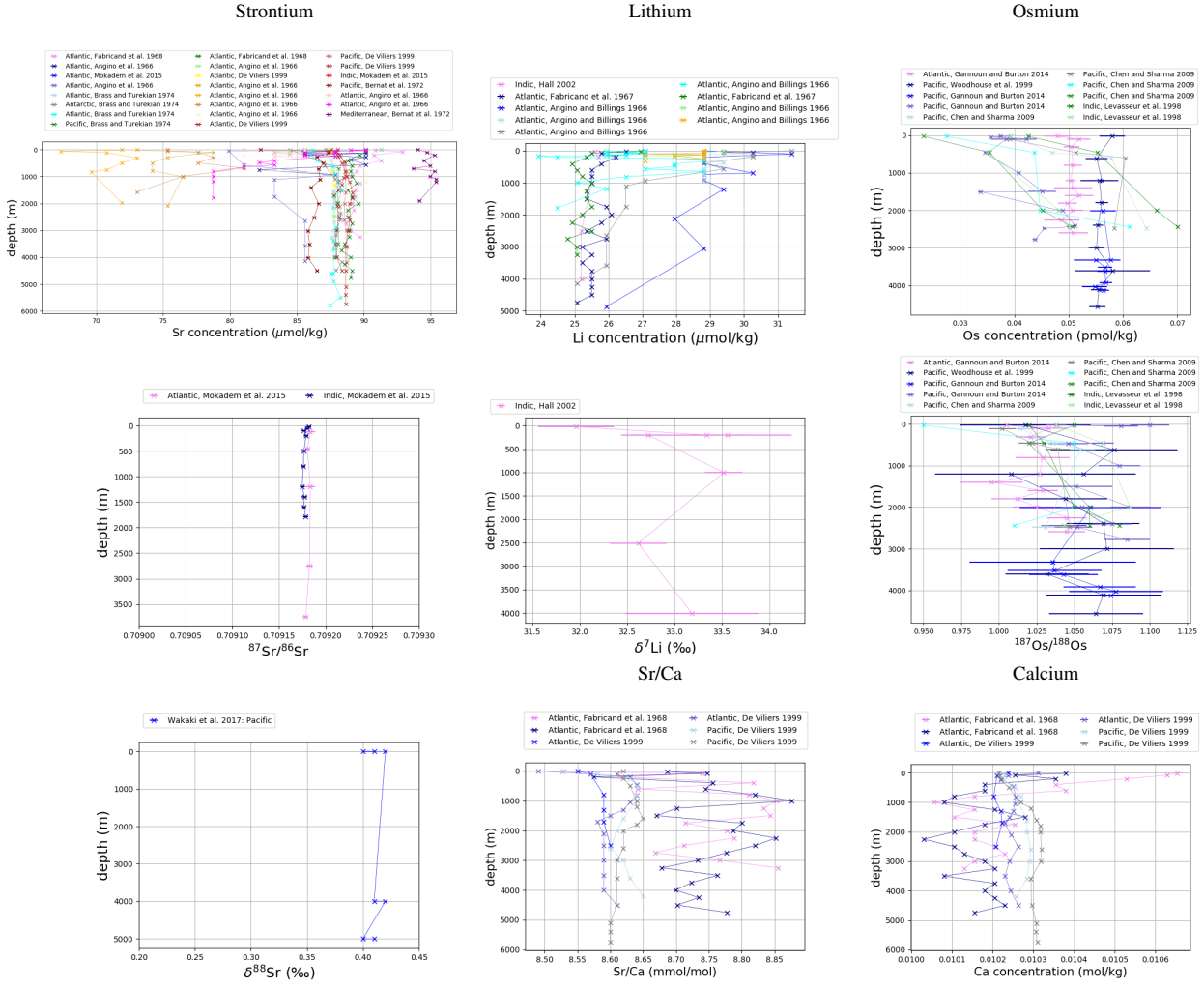

Figure A1. Comparison of measured Sr, Li, Os and Ca profiles in seawater. Shown are composites of all available profiles of measured concentrations and isotopic compositions. Data are taken from Angino et al. (1966), Fabricand et al. (1967), Bernat et al. (1972), Brass and Turekian (1974), De Villiers (1999), Mokadem et al. (2015) and Wakaki et al. (2017) for Sr, Angino and Billings (1966), Fabricand et al. (1967), Chan (1987), Chan and Edmond (1988), You and Chan (1996), Moriguti and Nakamura (1998), Tomascak et al. (1999), James and Palmer (2000), Košler et al. (2001), Nishio and Nakai (2002), Hall, Bryant et al. (2003), Pistiner and Henderson (2003), Millot et al. (2004), Choi et al. (2010) and Lin et al. (2016) for Li, Levasseur et al. (1998), Woodhouse et al. (1999) and Gannoun and Burton (2014) for Os and Fabricand et al. (1967) and De Villiers (1999) for Sr/Ca and Ca.

https://doi.org/10.5194/gmd-2020-233
Preprint. Discussion started: 10 August 2020

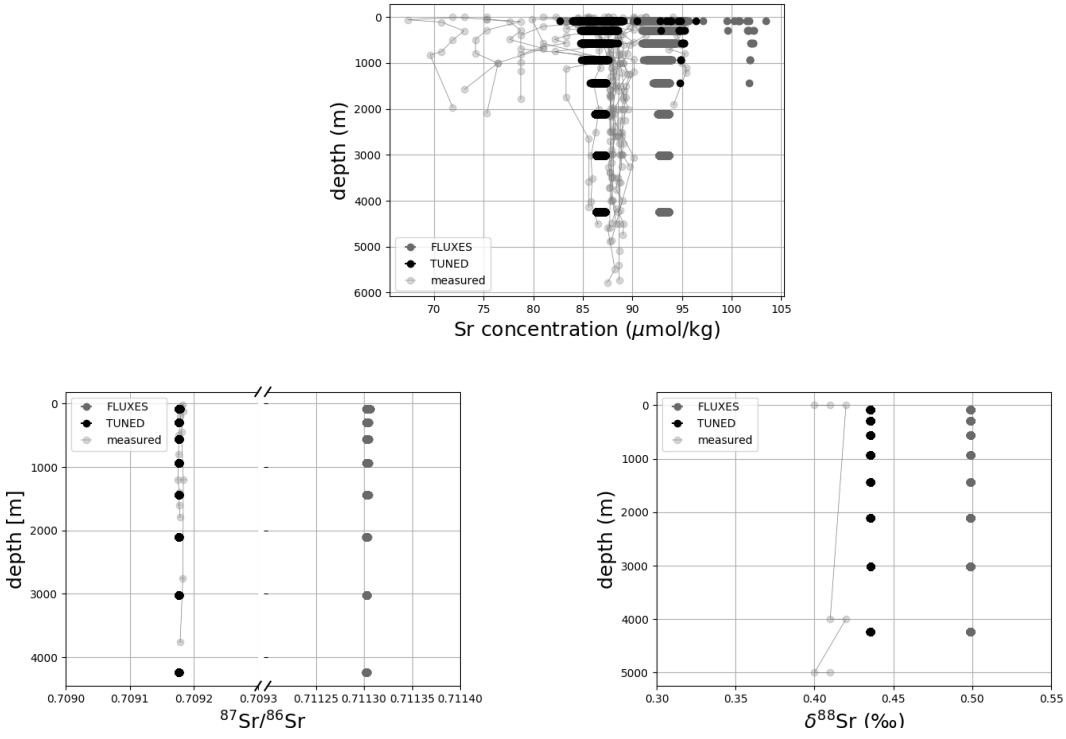

Figure A2. Comparison between measured and simulated Sr profiles in seawater. Shown are composites of all available measured Sr concentration and isotope ratio profiles and all profiles in the simulation. Data is taken from Angino et al. (1966), Fabricand et al. (1967), Bernat et al. (1972), Brass and Turekian (1974), De Villiers (1999) and Mokadem et al. (2015).

https://doi.org/10.5194/gmd-2020-233
Preprint. Discussion started: 10 August 2020

Geoscientific Model Development Discussions
Open Access
EGU

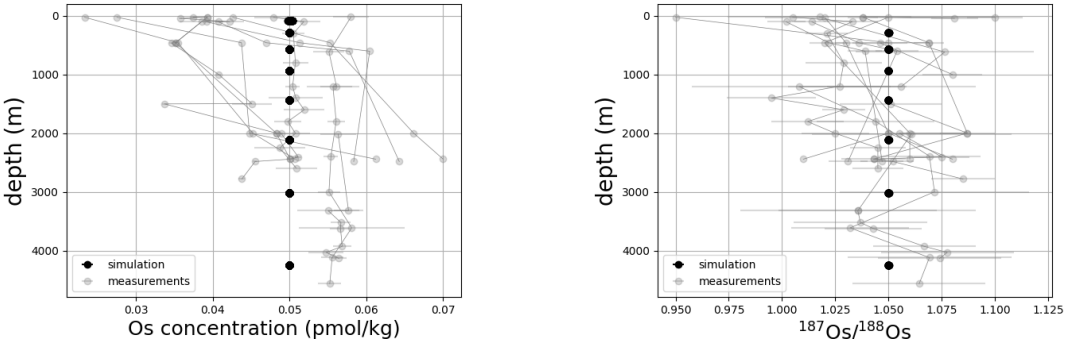

Figure A3. Comparison between measured and simulated Os vertical profiles in seawater. Shown are composites of all available measured Os concentration and isotope ratio profiles and all profiles in the simulation. Data is taken from Levasseur et al. (1998), Woodhouse et al. (1999) and Gannoun and Burton (2014).

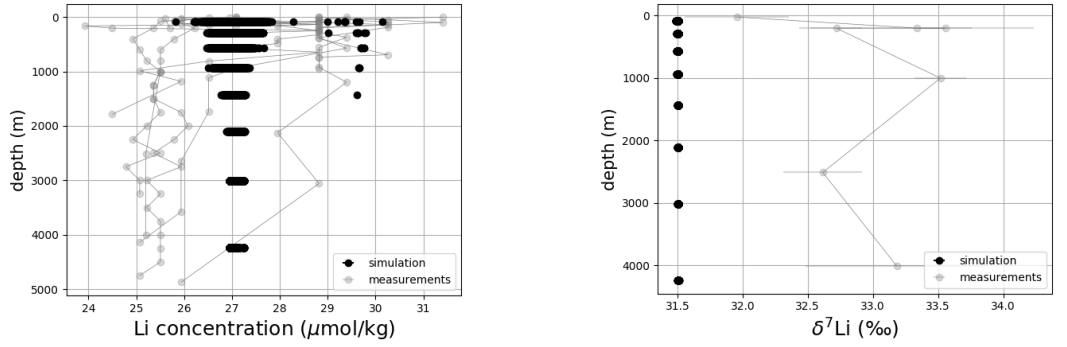

Figure A4. Comparison between measured and simulated Li profiles in seawater. Shown are composites of all available measured Li concentration and isotope ratio profiles and all profiles in the simulation. Data is taken from Angino and Billings (1966), Fabricand et al. (1967), Chan (1987), Chan and Edmond (1988), You and Chan (1996), Moriguti and Nakamura (1998), Tomascak et al. (1999), James and Palmer (2000), Košler et al. (2001), Nishio and Nakai (2002), Hall, Bryant et al. (2003), Pistiner and Henderson (2003), Millot et al. (2004), Choi et al. (2010) and Lin et al. (2016).

https://doi.org/10.5194/gmd-2020-233
Preprint. Discussion started: 10 August 2020

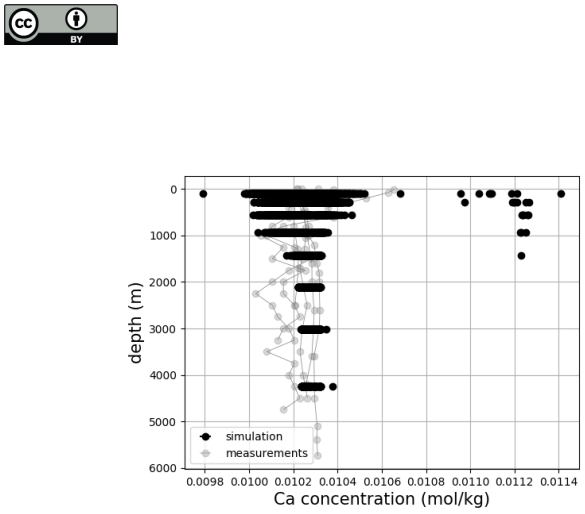

Geoscientific Model Development Discussions
Open Access
EGU

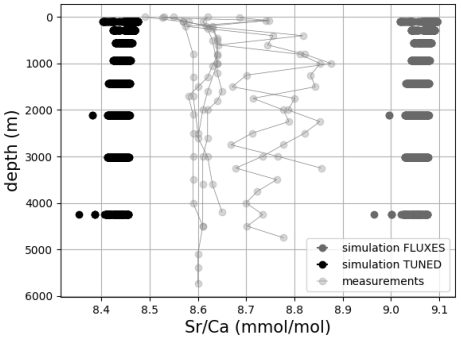

Figure A5. Comparison between measured and simulated Ca and Sr/Ca profiles in seawater. Shown are composites of all available measured concentration profiles and all profiles in the simulation. Data is taken from Fabricand et al. (1967), De Villiers (1999) and Fantle and Tipper (2014).

https://doi.org/10.5194/gmd-2020-233
Preprint. Discussion started: 10 August 2020

Geoscientific Model Development Discussions
Open Access
EGU

Appendix B: Site specific model-data comparison

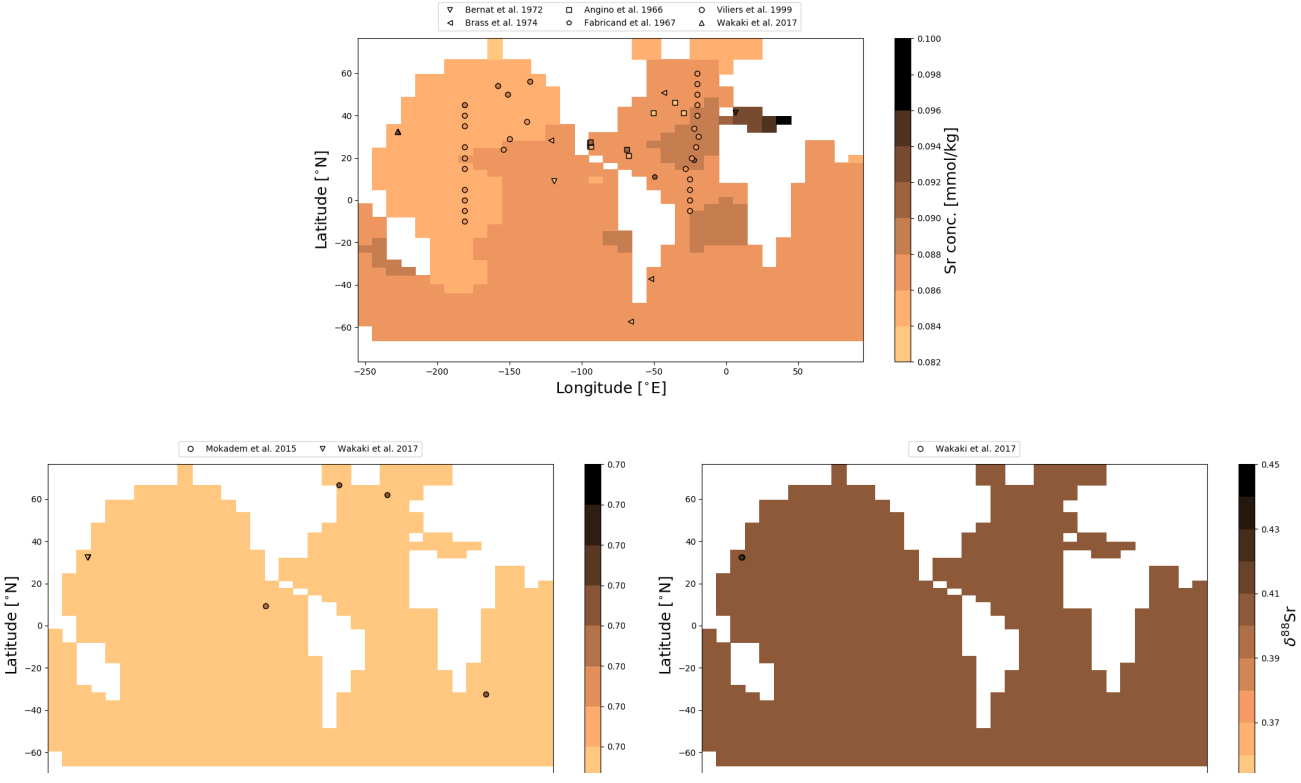

Figure C1. Comparison between measured and simulated Sr concentrations and isotopic composition in surface waters. Measurements are shown as symbols on the map, the colour indicating the respective value. Data is taken from Angino et al. (1966), Fabricand et al. (1967), Bernat et al. (1972), Brass and Turekian (1974), De Villiers (1999), Mokadem et al. (2015) and Wakaki et al. (2017).

Author contributions. The implementation of the Sr, Li and Ca cycles was conceived by AR, PPvS and MF and done by AR. The cGENIE Os cycle was conceived by MA, IP, AD and AR and implemented by MA and AR. MA compiled the observational data, validated the model output and produced the simulations and figures. MA prepared the manuscript with contributions from all co-authors.

Competing interests. No competing interests are present.

https://doi.org/10.5194/gmd-2020-233
Preprint. Discussion started: 10 August 2020

Acknowledgements. Furthermore, we would like to thank our funding bodies: M.A. was supported by the NERC GW4+ DTP and the Natural Environment Research Council [NE/L002434/1]. S.E.G. was supported by NERC grants NE/L011050/1 and NE/P01903X/1 while working on this manuscript. FMM was supported by a NERC standard grant (NE/N011112/1).

https://doi.org/10.5194/gmd-2020-233
Preprint. Discussion started: 10 August 2020

References

Allègre, C. J., Louvat, P., Gaillardet, J., Meynadier, L., Rad, S., and Capmas, F.: The fundamental role of island arc weathering in the oceanic Sr isotope budget, Earth and Planetary Science Letters, 292, 51–56, https://doi.org/10.1016/j.epsl.2010.01.019, http://www.sciencedirect.com/science/article/pii/S0012821X10000488, 2010.

Angino, E. E. and Billings, G. K.: Lithium content of sea water by atomic absorption spectrometry, Geochimica et Cosmochimica Acta, 30, 153–158, https://doi.org/10.1016/0016-7037(66)90104-9, http://www.sciencedirect.com/science/article/pii/0016703766901049, 1966.

Angino, E. E., Billings, G. K., and Andersen, N.: Observed variations in the strontium concentration of sea water, Chemical Geology, 1, 145–153, https://doi.org/10.1016/0009-2541(66)90013-1, http://www.sciencedirect.com/science/article/pii/0009254166900131, 1966.

Baskaran, M.: Handbook of environmental isotope geochemistry, Springer Science & Business Media, 2011.

Basu, A. R., Jacobsen, S. B., Poreda, R. J., Dowling, C. B., and Aggarwal, P. K.: Large groundwater strontium flux to the oceans from the Bengal Basin and the marine strontium isotope record, Science, 293, 1470–1473, https://doi.org/10.1126/science.1060524, https://science.sciencemag.org/content/293/5534/1470, 2001.

Bauer, K. W., Zeebe, R. E., and Wortmann, U. G.: Quantifying the volcanic emissions which triggered Oceanic Anoxic Event 1a and their effect on ocean acidification, Sedimentology, 64, 204–214, https://doi.org/10.1111/sed.12335, https://onlinelibrary.wiley.com/doi/abs/10.1111/sed.12335, 2017.

Beck, A. J., Charette, M. A., Cochran, J. K., Gonneea, M. E., and Peucker-Ehrenbrink, B.: Dissolved strontium in the subterranean estuary–implications for the marine strontium isotope budget, Geochimica et Cosmochimica Acta, 117, 33–52, https://doi.org/10.1016/j.gca.2013.03.021, http://www.sciencedirect.com/science/article/pii/S0016703713001774, 2013.

Bernat, M., Church, T., and Allegre, C. J.: Barium and strontium concentrations in Pacific and Mediterranean sea water profiles by direct isotope dilution mass spectrometry, Earth and planetary science letters, 16, 75–80, https://doi.org/10.1016/0012-821X(72)90238-5, http://www.sciencedirect.com/science/article/pii/0012821X72902385, 1972.

Berner, E. K. and Berner, R. A.: Global environment: water, air, and geochemical cycles, Princeton University Press, 2012.

Berner, R.: GEOCARB II: a revised model of atmospheric CO_2 levels over Phanerozoic time, Science, 249, 1382–1386, 1994.

Blättler, C. L., Jenkyns, H. C., Reynard, L. M., and Henderson, G. M.: Significant increases in global weathering during Oceanic Anoxic Events 1a and 2 indicated by calcium isotopes, Earth and Planetary Science Letters, 309, 77–88, https://doi.org/10.1016/j.epsl.2011.06.029, http://www.sciencedirect.com/science/article/pii/S0012821X11004006, 2011.

Blättler, C. L., Henderson, G. M., and Jenkyns, H. C.: Explaining the Phanerozoic Ca isotope history of seawater, Geology, 40, 843–846, https://doi.org/10.1130/G33191.1, https://doi.org/10.1130/G33191.1, 2012.

Böhm, F., Eisenhauer, A., Tang, J., Dietzel, M., Krabbenhöft, A., Kisakürek, B., and Horn, C.: Strontium isotope fractionation of planktic foraminifera and inorganic calcite, Geochimica et Cosmochimica Acta, 93, 300–314, https://doi.org/10.1016/j.gca.2012.04.038, http://www.sciencedirect.com/science/article/pii/S0016703712002438, 2012.

Bottini, C., Cohen, A. S., Erba, E., Jenkyns, H. C., and Coe, A. L.: Osmium-isotope evidence for volcanism, weathering, and ocean mixing during the early Aptian OAE 1a, Geology, 40, 583–586, https://doi.org/10.1130/G33140.1, https://doi.org/10.1130/G33140.1, 2012.

Brady, P. V.: The effect of silicate weathering on global temperature and atmospheric CO_2, Journal of Geophysical Research: Solid Earth, 96, 18 101–18 106, https://doi.org/10.1029/91JB01898, https://agupubs.onlinelibrary.wiley.com/doi/abs/10.1029/91JB01898, 1991.

Brady, P. V. and Gíslason, S. R.: Seafloor weathering controls on atmospheric CO_2 and global climate, Geochimica et Cosmochimica Acta, 61, 965–973, https://doi.org/10.1016/S0016-7037(96)00385-7, 1997.

https://doi.org/10.5194/gmd-2020-233
Preprint. Discussion started: 10 August 2020

Brass, G. W. and Turekian, K. K.: Strontium distribution in GEOSECS oceanic profiles, Earth and Planetary Science Letters, 23, 141–148, https://doi.org/10.1016/0012-821X(74)90041-7, http://www.sciencedirect.com/science/article/pii/0012821X74900417, 1974.

Broecker, W. and Peng, T.: Tracers in the Sea, Lamont-Doherty geological observatory, Palisades, New York, p. 690, https://doi.org/10.1017/S0033822200005221, 1982.

Bryant, C. J., McCulloch, M. T., and Bennett, V. C.: Impact of matrix effects on the accurate measurement of Li isotope ratios by inductively coupled plasma mass spectrometry (MC-ICP-MS) under "cold" plasma conditions, Journal of Analytical Atomic Spectrometry, 18, 734–737, https://doi.org/10.1039/B212083F, http://dx.doi.org/10.1039/B212083F, 2003.

Burton, K. W., Gannoun, A., and Parkinson, I. J.: Climate driven glacial–interglacial variations in the osmium isotope composition of seawater recorded by planktic foraminifera, Earth and Planetary Science Letters, 295, 58–68, https://doi.org/10.1016/j.epsl.2010.03.026, http://www.sciencedirect.com/science/article/pii/S0012821X10002074, 2010.

Campbell, I. H. and Allen, C. M.: Formation of supercontinents linked to increases in atmospheric oxygen, Nature Geoscience, 1, 554, https://doi.org/10.1038/ngeo259, https://doi.org/10.1038/ngeo259, 2008.

Carignan, J., Cardinal, D., Eisenhauer, A., Galy, A., Rehkamper, M., Wombacher, F., and Vigier, N.: A reflection on Mg, Cd, Ca, Li and Si isotopic measurements and related reference materials, Geostandards and Geoanalytical Research, 28, 139–148, https://doi.org/10.1111/j.1751-908X.2004.tb01050.x, https://onlinelibrary.wiley.com/doi/abs/10.1111/j.1751-908X.2004.tb01050.x, 2004.

Chan, L., Edmond, J., Thompson, G., and Gillis, K.: Lithium isotopic composition of submarine basalts: implications for the lithium cycle in the oceans, Earth and Planetary Science Letters, 108, 151–160, https://doi.org/10.1016/0012-821X(92)90067-6, http://www.sciencedirect.com/science/article/pii/0012821X92900676, 1992.

Chan, L. H.: Lithium isotope analysis by thermal ionization mass spectrometry of lithium tetraborate, Analytical Chemistry, 59, 2662–2665, https://doi.org/10.1021/ac00149a007, https://doi.org/10.1021/ac00149a007, 1987.

Chan, L.-H. and Edmond, J. M.: Variation of lithium isotope composition in the marine environment: A preliminary report, Geochimica et Cosmochimica Acta, 52, 1711–1717, https://doi.org/10.1016/0016-7037(88)90239-6, http://www.sciencedirect.com/science/article/pii/0016703788902396, 1988.

Choi, M. S., Shin, H. S., and Kil, Y. W.: Precise determination of lithium isotopes in seawater using MC-ICP-MS, Microchemical Journal, 95, 274–278, https://doi.org/10.1016/j.microc.2009.12.013, http://www.sciencedirect.com/science/article/pii/S0026265X09002306, 2010.

Clergue, C., Dellinger, M., Buss, H., Gaillardet, J., Benedetti, M., and Dessert, C.: Influence of atmospheric deposits and secondary minerals on Li isotopes budget in a highly weathered catchment, Guadeloupe (Lesser Antilles), Chemical Geology, 414, 28–41, https://doi.org/10.1016/j.chemgeo.2015.08.015, http://www.sciencedirect.com/science/article/pii/S0009254115300152, 2015.

Cocker, J., Griffin, B., and Muehlenbachs, K.: Oxygen and carbon isotope evidence for seawater-hydrothermal alteration of the Macquarie Island ophiolite, Earth and Planetary Science Letters, 61, 112–122, 1982.

Colbourn, G., Ridgwell, A., and Lenton, T.: The rock geochemical model (RokGeM) v0. 9, Geoscientific Model Development, 6, 1543–1573, https://doi.org/10.5194/gmd-6-1543-2013, 2013.

Dąbek, J. and Halas, S.: Physical foundations of rhenium-osmium method-a review, Geochronometria, 27, 23–26, https://doi.org/10.2478/v10003-007-0011-4, https://content.sciendo.com/view/journals/geochr/27/-1/article-p23.xml, 2007.

De Villiers, S.: Seawater strontium and Sr/Ca variability in the Atlantic and Pacific oceans, Earth and Planetary Science Letters, 171, 623–634, https://doi.org/10.1016/S0012-821X(99)00174-0, http://www.sciencedirect.com/science/article/pii/S0012821X99001740, 1999.

https://doi.org/10.5194/gmd-2020-233
Preprint. Discussion started: 10 August 2020

Death, R., Wadham, J., Monteiro, F., Le Brocq, A., Tranter, M., Ridgwell, A., Dutkiewicz, S., and Raiswell, R.: Antarctic ice sheet fertilises the Southern Ocean, Biogeosciences, 11, 2635–2643, https://doi.org/10.5194/bg-11-2635-2014, 2014.

Dellinger, M., Gaillardet, J., Bouchez, J., Calmels, D., Louvat, P., Dosseto, A., Gorge, C., Alanoca, L., and Maurice, L.: Riverine Li isotope fractionation in the Amazon River basin controlled by the weathering regimes, Geochimica et Cosmochimica Acta, 164, 71–93, https://doi.org/10.1016/j.gca.2015.04.042, http://www.sciencedirect.com/science/article/pii/S0016703715002483, 2015.

Dellinger, M., West, A. J., Paris, G., Adkins, J. F., von Strandmann, P. A. P., Ullmann, C. V., Eagle, R. A., Freitas, P., Bagard, M.-L., Ries, J. B., et al.: The Li isotope composition of marine biogenic carbonates: Patterns and Mechanisms, Geochimica et Cosmochimica Acta, 236, 315–335, https://doi.org/10.1016/j.gca.2018.03.014, http://www.sciencedirect.com/science/article/pii/S0016703718301650, 2018.

DePaolo, D. J.: Calcium isotopic variations produced by biological, kinetic, radiogenic and nucleosynthetic processes, Reviews in mineralogy and geochemistry, 55, 255–288, https://doi.org/10.2138/gsrmg.55.1.255, https://doi.org/10.2138/gsrmg.55.1.255, 2004.

DePaolo, D. J.: Surface kinetic model for isotopic and trace element fractionation during precipitation of calcite from aqueous solutions, Geochimica et cosmochimica acta, 75, 1039–1056, https://doi.org/10.1016/j.gca.2010.11.020, http://www.sciencedirect.com/science/article/pii/S0016703710006599, 2011.

Derry, L. A.: Geochemistry: A glacial hangover, Nature, 458, 417, https://doi.org/10.1038/458417a, 2009.

Dickson, A. J., Cohen, A. S., Coe, A. L., Davies, M., Shcherbinina, E. A., and Gavrilov, Y. O.: Evidence for weathering and volcanism during the PETM from Arctic Ocean and Peri-Tethys osmium isotope records, Palaeogeography, Palaeoclimatology, Palaeoecology, 438, 300–307, https://doi.org/10.1016/j.palaeo.2015.08.019, http://www.sciencedirect.com/science/article/pii/S0031018215004551, 2015.

Dubin, A. and Peucker-Ehrenbrink, B.: The importance of organic-rich shales to the geochemical cycles of rhenium and osmium, Chemical Geology, 403, 111–120, https://doi.org/10.1016/j.chemgeo.2015.03.010, http://www.sciencedirect.com/science/article/pii/S0009254115001448, 2015.

Edwards, N. R. and Marsh, R.: Uncertainties due to transport-parameter sensitivity in an efficient 3-D ocean-climate model, Climate dynamics, 24, 415–433, https://doi.org/10.1007/s00382-004-0508-8, 2005.

Elderfield, H.: Strontium isotope stratigraphy, Palaeogeography, palaeoclimatology, palaeoecology, 57, 71–90, https://doi.org/10.1016/0031-0182(86)90007-6, http://www.sciencedirect.com/science/article/pii/0031018286900076, 1986.

Elderfield, H. and Gieskes, J. M.: Sr isotopes in interstitial waters of marine sediments from Deep Sea Drilling Project cores, Nature, 300, 493, https://doi.org/10.1038/300493a0, 1982.

Erba, E., Bottini, C., Weissert, H. J., and Keller, C. E.: Calcareous nannoplankton response to surface-water acidification around Oceanic Anoxic Event 1a, Science, 329, 428–432, https://doi.org/10.1126/science.1188886, https://science.sciencemag.org/content/329/5990/428, 2010.

Fabricand, B., Imbimbo, E., and Brey, M.: Atomic absorption analyses for Ca, Li, Mg, K, Rb, and Sr at two Atlantic Ocean stations, in: Deep Sea Research and Oceanographic Abstracts, vol. 14, pp. 785–789, Elsevier, https://doi.org/10.1016/S0011-7471(67)80014-7, http://www.sciencedirect.com/science/article/pii/S0011747167800147, 1967.

Fantle, M. S. and Tipper, E. T.: Calcium isotopes in the global biogeochemical Ca cycle: Implications for development of a Ca isotope proxy, Earth-Science Reviews, 129, 148–177, https://doi.org/10.1016/j.earscirev.2013.10.004, http://www.sciencedirect.com/science/article/pii/S0012825213001700, 2014.

Fantle, M. S., Tollerud, H., Eisenhauer, A., and Holmden, C.: The Ca isotopic composition of dust-producing regions: Measurements of surface sediments in the Black Rock Desert, Nevada, Geochimica et Cosmochimica Acta, 87, 178–193, https://doi.org/10.1016/j.gca.2012.03.037, http://www.sciencedirect.com/science/article/pii/S0016703712001895, 2012.

https://doi.org/10.5194/gmd-2020-233
Preprint. Discussion started: 10 August 2020

Fantle, M. S., Barnes, B. D., and Lau, K. V.: The Role of Diagenesis in Shaping the Geochemistry of the Marine Carbonate Record., Annual Review of Earth and Planetary Sciences, 48, 549–583, https://doi.org/10.1146/annurev-earth-073019-060021, https://doi.org/10.1146/annurev-earth-073019-060021, 2020.

Farkaš, J., Böhm, F., Wallmann, K., Blenkinsop, J., Eisenhauer, A., Van Geldern, R., Munnecke, A., Voigt, S., and Veizer, J.: Calcium isotope record of Phanerozoic oceans: Implications for chemical evolution of seawater and its causative mechanisms, Geochimica et Cosmochimica Acta, 71, 5117–5134, https://doi.org/10.1016/j.gca.2007.09.004, http://www.sciencedirect.com/science/article/pii/S0016703707005133, 2007.

Faure, G. and Mensing, T. M.: Isotopes: principles and applications, Wiley-Blackwell, 2005.

Fietzke, J. and Eisenhauer, A.: Determination of temperature-dependent stable strontium isotope ($^{88}Sr/^{86}Sr$) fractionation via bracketing standard MC-ICP-MS, Geochemistry, Geophysics, Geosystems, 7, https://doi.org/10.1029/2006GC001243, https://agupubs.onlinelibrary.wiley.com/doi/abs/10.1029/2006GC001243, 2006.

Finlay, A. J., Selby, D., and Gröcke, D. R.: Tracking the Hirnantian glaciation using Os isotopes, Earth and Planetary Science Letters, 293, 339–348, https://doi.org/10.1016/j.epsl.2010.02.049, http://www.sciencedirect.com/science/article/pii/S0012821X10001603, 2010.

Fries, D. M., James, R. H., Dessert, C., Bouchez, J., Beaumais, A., and Pearce, C. R.: The response of Li and Mg isotopes to rain events in a highly-weathered catchment, Chemical Geology, 519, 68–82, https://doi.org/10.1016/j.chemgeo.2019.04.023, http://www.sciencedirect.com/science/article/pii/S0009254119302062, 2019.

Gannoun, A. and Burton, K. W.: High precision osmium elemental and isotope measurements of North Atlantic seawater, Journal of Analytical Atomic Spectrometry, 29, 2330–2342, https://doi.org/10.1039/C4JA00265B, 2014.

Georg, R., West, A., Vance, D., Newman, K., and Halliday, A. N.: Is the marine osmium isotope record a probe for CO_2 release from sedimentary rocks?, Earth and Planetary Science Letters, 367, 28–38, https://doi.org/10.1016/j.epsl.2013.02.018, http://www.sciencedirect.com/science/article/pii/S0012821X1300085X, 2013.

Goddéris, Y. and François, L.: The Cenozoic evolution of the strontium and carbon cycles: relative importance of continental erosion and mantle exchanges, Chemical Geology, 126, 169–190, https://doi.org/10.1016/0009-2541(95)00117-3, http://www.sciencedirect.com/science/article/pii/0009254195001173, 1995.

Goldschmidt, V. M.: Der Stoffwechsel der Erde, Zeitschrift für Elektrochemie und angewandte physikalische Chemie, 28, 411–421, https://doi.org/10.1002/bbpc.19220281906, https://onlinelibrary.wiley.com/doi/abs/10.1002/bbpc.19220281906, 1922.

Gou, L.-F., Jin, Z., von Strandmann, P. A. P., Li, G., Qu, Y.-X., Xiao, J., Deng, L., and Galy, A.: Li isotopes in the middle Yellow River: Seasonal variability, sources and fractionation, Geochimica et Cosmochimica Acta, 248, 88–108, https://doi.org/10.1016/j.gca.2019.01.007, http://www.sciencedirect.com/science/article/pii/S0016703719300201, 2019.

Griffith, E. M., Paytan, A., Caldeira, K., Bullen, T. D., and Thomas, E.: A dynamic marine calcium cycle during the past 28 million years, Science, 322, 1671–1674, https://doi.org/10.1126/science.1163614, https://science.sciencemag.org/content/322/5908/1671, 2008.

Hall, J. M.: Barium and lithium in foraminifera: Glacial-interglacial changes in the North Atlantic, LSU Doctoral Dissertations.

Hall, J. M. and Chan, L.-H.: Li/Ca in multiple species of benthic and planktonic foraminifera: thermocline, latitudinal, and glacial-interglacial variation, Geochimica et Cosmochimica Acta, 68, 529–545, https://doi.org/10.1016/S0016-7037(03)00451-4, http://www.sciencedirect.com/science/article/pii/S0016703703004514, 2004.

Hall, J. M., Chan, L.-H., McDonough, W. F., and Turekian, K. K.: Determination of the lithium isotopic composition of planktic foraminifera and its application as a paleo-seawater proxy, Marine Geology, 217, 255–265, https://doi.org/10.1016/j.margeo.2004.11.015, http://www.sciencedirect.com/science/article/pii/S0025322705000526, 2005.

https://doi.org/10.5194/gmd-2020-233
Preprint. Discussion started: 10 August 2020

Hathorne, E. C. and James, R. H.: Temporal record of lithium in seawater: A tracer for silicate weathering?, Earth and Planetary Science Letters, 246, 393–406, https://doi.org/10.1016/j.epsl.2006.04.020, http://www.sciencedirect.com/science/article/pii/S0012821X06003086, 2006.

Henchiri, S., Gaillardet, J., Dellinger, M., Bouchez, J., and Spencer, R. G.: Riverine dissolved lithium isotopic signatures in low-relief central Africa and their link to weathering regimes, Geophysical Research Letters, 43, 4391–4399, https://doi.org/10.1002/2016GL067711, https://agupubs.onlinelibrary.wiley.com/doi/abs/10.1002/2016GL067711, 2016.

Heuser, A., Eisenhauer, A., Gussone, N., Bock, B., Hansen, B., and Nägler, T. F.: Measurement of calcium isotopes (δ44Ca) using a multicollector TIMS technique, International Journal of Mass Spectrometry, 220, 385–397, https://doi.org/10.1016/S1387-3806(02)00838-2, http://www.sciencedirect.com/science/article/pii/S1387380602008382, 2002.

Hindshaw, R. S., Reynolds, B. C., Wiederhold, J. G., Kiczka, M., Kretzschmar, R., and Bourdon, B.: Calcium isotope fractionation in alpine plants, Biogeochemistry, 112, 373–388, https://doi.org/10.1007/s10533-012-9732-1, 2013.

Hindshaw, R. S., Tosca, R., Goût, T. L., Farnan, I., Tosca, N. J., and Tipper, E. T.: Experimental constraints on Li isotope fractionation during clay formation, Geochimica et Cosmochimica Acta, 250, 219–237, https://doi.org/10.1016/j.gca.2019.02.015, http://www.sciencedirect.com/science/article/pii/S0016703719300924, 2019.

Hodell, D. A., Mueller, P. A., McKenzie, J. A., and Mead, G. A.: Strontium isotope stratigraphy and geochemistry of the late Neogene ocean, Earth and Planetary Science Letters, 92, 165–178, https://doi.org/10.1016/0012-821X(89)90044-7, http://www.sciencedirect.com/science/article/pii/0012821X89900447, 1989.

Hodell, D. A., Mead, G. A., and Mueller, P. A.: Variation in the strontium isotopic composition of seawater (8 Ma to present): Implications for chemical weathering rates and dissolved fluxes to the oceans, Chemical Geology: Isotope Geoscience section, 80, 291–307, https://doi.org/10.1016/0168-9622(90)90011-Z, http://www.sciencedirect.com/science/article/pii/016896229090011Z, 1990.

Holmden, C., Papanastassiou, D., Blanchon, P., and Evans, S.: $\delta^{44/40}$Ca variability in shallow water carbonates and the impact of submarine groundwater discharge on Ca-cycling in marine environments, Geochimica et Cosmochimica Acta, 83, 179–194, https://doi.org/10.1016/j.gca.2011.12.031, http://www.sciencedirect.com/science/article/pii/S0016703711007666, 2012.

Hooper, J., Mayewski, P., Marx, S., Henson, S., Potocki, M., Sneed, S., Handley, M., Gassó, S., Fischer, M., and Saunders, K. M.: Examining links between dust deposition and phytoplankton response using ice cores, Aeolian Research, 36, 45–60, https://doi.org/10.1016/j.aeolia.2018.11.001, http://www.sciencedirect.com/science/article/pii/S1875963718301101, 2019.

Huh, Y., Chan, L.-H., Zhang, L., and Edmond, J. M.: Lithium and its isotopes in major world rivers: implications for weathering and the oceanic budget, Geochimica et Cosmochimica Acta, 62, 2039–2051, https://doi.org/10.1016/S0016-7037(98)00126-4, http://www.sciencedirect.com/science/article/pii/S0016703798001264, 1998.

Hülse, D., Arndt, S., and Ridgwell, A.: Mitigation of extreme Ocean Anoxic Event conditions by organic matter sulfurization, Paleoceanography and Paleoclimatology, 34, https://doi.org/10.1029/2018PA003470, https://agupubs.onlinelibrary.wiley.com/doi/abs/10.1029/2018PA003470, 2019.

Jaffe, L. A., Peucker-Ehrenbrink, B., and Petsch, S. T.: Mobility of rhenium, platinum group elements and organic carbon during black shale weathering, Earth and Planetary Science Letters, 198, 339–353, https://doi.org/10.1016/S0012-821X(02)00526-5, http://www.sciencedirect.com/science/article/pii/S0012821X02005265, 2002.

James, R. H. and Palmer, M. R.: The lithium isotope composition of international rock standards, Chemical Geology, 166, 319–326, https://doi.org/10.1016/S0009-2541(99)00217-X, http://www.sciencedirect.com/science/article/pii/S000925419900217X, 2000.

https://doi.org/10.5194/gmd-2020-233
Preprint. Discussion started: 10 August 2020

Jenkyns, H. C.: Geochemistry of oceanic anoxic events, Geochemistry, Geophysics, Geosystems, 11, https://doi.org/10.1029/2009GC002788, https://agupubs.onlinelibrary.wiley.com/doi/abs/10.1029/2009GC002788, 2010.

John, E. H., Wilson, J. D., Pearson, P. N., and Ridgwell, A.: Temperature-dependent remineralization and carbon cycling in the warm Eocene oceans, Palaeogeography, Palaeoclimatology, Palaeoecology, 413, 158–166, https://doi.org/10.1016/j.palaeo.2014.05.019, http://www.sciencedirect.com/science/article/pii/S0031018214002685, 2014.

Kasemann, S. A., Hawkesworth, C. J., Prave, A. R., Fallick, A. E., and Pearson, P. N.: Boron and calcium isotope composition in Neoproterozoic carbonate rocks from Namibia: evidence for extreme environmental change, Earth and Planetary Science Letters, 231, 73–86, https://doi.org/10.1016/j.epsl.2004.12.006, http://www.sciencedirect.com/science/article/pii/S0012821X04007113, 2005.

Kasemann, S. A., Schmidt, D. N., Pearson, P. N., and Hawkesworth, C. J.: Biological and ecological insights into Ca isotopes in planktic foraminifers as a palaeotemperature proxy, Earth and Planetary Science Letters, 271, 292–302, https://doi.org/10.1016/j.epsl.2008.04.007, http://www.sciencedirect.com/science/article/pii/S0012821X08002598, 2008.

Kasemann, S. A., von Strandmann, P. A. P., Prave, A. R., Fallick, A. E., Elliott, T., and Hoffmann, K.-H.: Continental weathering following a Cryogenian glaciation: Evidence from calcium and magnesium isotopes, Earth and Planetary Science Letters, 396, 66–77, https://doi.org/10.1016/j.epsl.2014.03.048, http://www.sciencedirect.com/science/article/pii/S0012821X14002003, 2014.

Kent, D. V. and Muttoni, G.: Modulation of Late Cretaceous and Cenozoic climate by variable drawdown of atmospheric pCO_2 from weathering of basaltic provinces on continents drifting through the equatorial humid belt, Climate of the Past, 9, 525–546, https://doi.org/10.5194/cpd-8-4513-2012, 2013.

Kısakűrek, B., James, R. H., and Harris, N. B.: Li and δ7Li in Himalayan rivers: proxies for silicate weathering?, Earth and Planetary Science Letters, 237, 387–401, https://doi.org/10.1016/j.epsl.2005.07.019, http://www.sciencedirect.com/science/article/pii/S0012821X05005005, 2005.

Košler, J., Kučera, M., and Sylvester, P.: Precise measurement of Li isotopes in planktonic foraminiferal tests by quadrupole ICPMS, Chemical Geology, 181, 169–179, https://doi.org/10.1016/S0009-2541(01)00280-7, http://www.sciencedirect.com/science/article/pii/S0009254101002807, 2001.

Krabbenhöft, A.: Stable Strontium Isotope ($\delta^{88/86}$Sr) Fractionation in the Marine Realm: A Pilot Study, Ph.D. thesis, Christian-Albrechts Universität Kiel, 2011.

Krabbenhöft, A., Eisenhauer, A., Böhm, F., Vollstaedt, H., Fietzke, J., Liebetrau, V., Augustin, N., Peucker-Ehrenbrink, B., Müller, M., Horn, C., et al.: Constraining the marine strontium budget with natural strontium isotope fractionations (^{87}Sr/^{86}Sr, $\delta^{88/86}$Sr) of carbonates, hydrothermal solutions and river waters, Geochimica et Cosmochimica Acta, 74, 4097–4109, https://doi.org/10.1016/j.gca.2010.04.009, http://www.sciencedirect.com/science/article/pii/S0016703710001845, 2010.

Krissansen-Totton, J. and Catling, D. C.: Constraining climate sensitivity and continental versus seafloor weathering using an inverse geological carbon cycle model, Nature communications, 8, 1–15, https://doi.org/10.1038/ncomms15423, 2017.

Kristall, B., Jacobson, A. D., and Hurtgen, M. T.: Modeling the paleo-seawater radiogenic strontium isotope record: A case study of the Late Jurassic-Early Cretaceous, Palaeogeography, palaeoclimatology, palaeoecology, 472, 163–176, https://doi.org/10.1016/j.palaeo.2017.01.048, http://www.sciencedirect.com/science/article/pii/S0031018216305491, 2017.

Kump, L. R. and Barley, M. E.: Increased subaerial volcanism and the rise of atmospheric oxygen 2.5 billion years ago, Nature, 448, 1033, https://doi.org/10.1038/nature06058, 2007.

https://doi.org/10.5194/gmd-2020-233
Preprint. Discussion started: 10 August 2020

Lemarchand, E., Chabaux, F., Vigier, N., Millot, R., and Pierret, M.-C.: Lithium isotope systematics in a forested granitic catchment (Strengbach, Vosges Mountains, France), Geochimica et Cosmochimica Acta, 74, 4612–4628, https://doi.org/10.1016/j.gca.2010.04.057, http://www.sciencedirect.com/science/article/pii/S0016703710002425, 2010.

Levasseur, S., Birck, J.-L., and Allègre, C. J.: Direct measurement of femtomoles of osmium and the $^{187}Os/^{186}Os$ ratio in seawater, Science, 282, 272–274, https://doi.org/10.1126/science.282.5387.272, https://science.sciencemag.org/content/282/5387/272, 1998.

Lin, J., Liu, Y., Hu, Z., Yang, L., Chen, K., Chen, H., Zong, K., and Gao, S.: Accurate determination of lithium isotope ratios by MC-ICP-MS without strict matrix-matching by using a novel washing method, Journal of Analytical Atomic Spectrometry, 31, 390–397, https://doi.org/10.1039/C5JA00231A, http://dx.doi.org/10.1039/C5JA00231A, 2016.

Lord, N. S., Ridgwell, A., Thorne, M., and Lunt, D.: An impulse response function for the "long tail" of excess atmospheric CO_2 in an Earth system model, Global Biogeochemical Cycles, 30, 2–17, https://doi.org/10.1002/2014GB005074, https://agupubs.onlinelibrary.wiley.com/doi/abs/10.1002/2014GB005074, 2016.

Loveley, M. R., Marcantonio, F., Wisler, M. M., Hertzberg, J. E., Schmidt, M. W., and Lyle, M.: Millennial-scale iron fertilization of the eastern equatorial Pacific over the past 100,000 years, Nature Geoscience, 10, 760, https://doi.org/10.1038/ngeo3024, 2017.

Lu, X., Kendall, B., Stein, H. J., and Hannah, J. L.: Temporal record of osmium concentrations and $^{187}Os/^{188}Os$ in organic-rich mudrocks: Implications for the osmium geochemical cycle and the use of osmium as a paleoceanographic tracer, Geochimica et Cosmochimica Acta, 216, 221–241, https://doi.org/10.1016/j.gca.2017.06.046, http://www.sciencedirect.com/science/article/pii/S0016703717304052, 2017.

Marriott, C. S., Henderson, G. M., Belshaw, N. S., and Tudhope, A. W.: Temperature dependence of δ^7Li, δ^{44}Ca and Li/Ca during growth of calcium carbonate, Earth and Planetary Science Letters, 222, 615–624, https://doi.org/10.1016/j.epsl.2004.02.031, http://www.sciencedirect.com/science/article/pii/S0012821X04001499, 2004.

Martin, J. H.: Glacial-interglacial CO_2 change: The iron hypothesis, Paleoceanography, 5, 1–13, https://doi.org/10.1029/PA005i001p00001, https://agupubs.onlinelibrary.wiley.com/doi/abs/10.1029/PA005i001p00001, 1990.

Martínez-Garcia, A., Rosell-Melé, A., Jaccard, S. L., Geibert, W., Sigman, D. M., and Haug, G. H.: Southern Ocean dust–climate coupling over the past four million years, Nature, 476, 312–315, https://doi.org/10.1038/nature10310, 2011.

Mason, E., Edmonds, M., and Turchyn, A. V.: Remobilization of crustal carbon may dominate volcanic arc emissions, Science, 357, 290–294, https://doi.org/10.1126/science.aan5049, https://science.sciencemag.org/content/357/6348/290, 2017.

Menzies, M. and Seyfried Jr, W.: Basalt-seawater interaction: trace element and strontium isotopic variations in experimentally altered glassy basalt, Earth and Planetary Science Letters, 44, 463–472, https://doi.org/10.1016/0012-821X(79)90084-0, 1979.

Milliman, J. D.: Production and accumulation of calcium carbonate in the ocean: budget of a nonsteady state, Global Biogeochemical Cycles, 7, 927–957, https://doi.org/10.1029/93GB02524, https://agupubs.onlinelibrary.wiley.com/doi/abs/10.1029/93GB02524, 1993.

Millot, R., Guerrot, C., and Vigier, N.: Accurate and high-precision measurement of lithium isotopes in two reference materials by MC-ICP-MS, Geostandards and Geoanalytical Research, 28, 153–159, https://doi.org/10.1111/j.1751-908X.2004.tb01052.x, https://onlinelibrary.wiley.com/doi/abs/10.1111/j.1751-908X.2004.tb01052.x, 2004.

Millot, R., Vigier, N., and Gaillardet, J.: Behaviour of lithium and its isotopes during weathering in the Mackenzie Basin, Canada, Geochimica et Cosmochimica Acta, 74, 3897–3912, https://doi.org/10.1016/j.gca.2010.04.025, http://www.sciencedirect.com/science/article/pii/S0016703710002103, 2010.

Mills, B., Daines, S. J., and Lenton, T. M.: Changing tectonic controls on the long-term carbon cycle from Mesozoic to present, Geochemistry, Geophysics, Geosystems, 15, 4866–4884, https://doi.org/10.1002/2014GC005530, https://agupubs.onlinelibrary.wiley.com/doi/abs/10.1002/2014GC005530, 2014.

https://doi.org/10.5194/gmd-2020-233
Preprint. Discussion started: 10 August 2020

Misra, S. and Froelich, P. N.: Lithium isotope history of Cenozoic seawater: changes in silicate weathering and reverse weathering, Science, 335, 818–823, https://doi.org/10.1126/science.1214697, https://science.sciencemag.org/content/335/6070/818, 2012.

Mokadem, F., Parkinson, I. J., Hathorne, E. C., Anand, P., Allen, J. T., and Burton, K. W.: High-precision radiogenic strontium isotope measurements of the modern and glacial ocean: Limits on glacial–interglacial variations in continental weathering, Earth and Planetary Science Letters, 415, 111–120, https://doi.org/10.1016/j.epsl.2015.01.036, http://www.sciencedirect.com/science/article/pii/S0012821X15000643, 2015.

Monteiro, F., Pancost, R., Ridgwell, A., and Donnadieu, Y.: Nutrients as the dominant control on the spread of anoxia and euxinia across the Cenomanian-Turonian oceanic anoxic event (OAE2): Model-data comparison, Paleoceanography, 27, https://doi.org/10.1029/2012PA002351, https://agupubs.onlinelibrary.wiley.com/doi/abs/10.1029/2012PA002351, 2012.

Moriguti, T. and Nakamura, E.: High-yield lithium separation and the precise isotopic analysis for natural rock and aqueous samples, Chemical Geology, 145, 91–104, https://doi.org/10.1016/S0009-2541(97)00163-0, http://www.sciencedirect.com/science/article/pii/S0009254197001630, 1998.

Müller, M. N., Krabbenhöft, A., Vollstaedt, H., Brandini, F., and Eisenhauer, A.: Stable isotope fractionation of strontium in coccolithophore calcite: Influence of temperature and carbonate chemistry, Geobiology, 16, 297–306, https://doi.org/10.1111/gbi.12276, https://onlinelibrary.wiley.com/doi/abs/10.1111/gbi.12276, 2018.

Murphy, M. J., Porcelli, D., von Strandmann, P. A. P., Hirst, C. A., Kutscher, L., Katchinoff, J. A., Mörth, C.-M., Maximov, T., and Andersson, P. S.: Tracing silicate weathering processes in the permafrost-dominated Lena River watershed using lithium isotopes, Geochimica et Cosmochimica Acta, 245, 154–171, https://doi.org/10.1016/j.gca.2018.10.024, http://www.sciencedirect.com/science/article/pii/S0016703718306100, 2019.

Nägler, T. F., Eisenhauer, A., Müller, A., Hemleben, C., and Kramers, J.: The δ44Ca-temperature calibration on fossil and cultured Globigerinoides sacculifer: New tool for reconstruction of past sea surface temperatures, Geochemistry, Geophysics, Geosystems, 1, https://doi.org/10.1029/2000GC000091, https://agupubs.onlinelibrary.wiley.com/doi/abs/10.1029/2000GC000091, 2000.

Nanne, J. A., Millet, M.-A., Burton, K. W., Dale, C. W., Nowell, G. M., and Williams, H. M.: High precision osmium stable isotope measurements by double spike MC-ICP-MS and N-TIMS, Journal of analytical atomic spectrometry, 32, 749–765, https://doi.org/10.1039/C6JA00406G, 2017.

Nishio, Y. and Nakai, S.: Accurate and precise lithium isotopic determinations of igneous rock samples using multi-collector inductively coupled plasma mass spectrometry, Analytica Chimica Acta, 456, 271–281, https://doi.org/10.1016/S0003-2670(02)00042-9, http://www.sciencedirect.com/science/article/pii/S0003267002000429, 2002.

Oxburgh, R.: Residence time of osmium in the oceans, Geochemistry, Geophysics, Geosystems, 2, https://doi.org/10.1029/2000GC000104, https://agupubs.onlinelibrary.wiley.com/doi/abs/10.1029/2000GC000104, 2001.

Panchuk, K., Ridgwell, A., and Kump, L.: Sedimentary response to Paleocene-Eocene Thermal Maximum carbon release: A model-data comparison, Geology, 36, 315–318, https://doi.org/10.1130/G24474A.1, https://doi.org/10.1130/G24474A.1, 2008.

Parkinson, I. J., Hammond, S. J., James, R. H., and Rogers, N. W.: High-temperature lithium isotope fractionation: Insights from lithium isotope diffusion in magmatic systems, Earth and Planetary Science Letters, 257, 609–621, https://doi.org/10.1016/j.epsl.2007.03.023, http://www.sciencedirect.com/science/article/pii/S0012821X07001793, 2007.

Pearce, C. R., Parkinson, I. J., Gaillardet, J., Charlier, B. L., Mokadem, F., and Burton, K. W.: Reassessing the stable ($\delta^{88/86}$Sr) and radiogenic (^{87}Sr/^{86}Sr) strontium isotopic composition of marine inputs, Geochimica et Cosmochimica Acta, 157, 125–146, https://doi.org/10.1016/j.gca.2015.02.029, http://www.sciencedirect.com/science/article/pii/S0016703715001222, 2015.

https://doi.org/10.5194/gmd-2020-233
Preprint. Discussion started: 10 August 2020

Penniston-Dorland, S., Liu, X.-M., and Rudnick, R. L.: Lithium isotope geochemistry, Reviews in Mineralogy and Geochemistry, 82, 165–217, https://doi.org/10.2138/rmg.2017.82.6, https://doi.org/10.2138/rmg.2017.82.6, 2017.

Percival, L., Witt, M., Mather, T., Hermoso, M., Jenkyns, H., Hesselbo, S., Al-Suwaidi, A., Storm, M., Xu, W., and Ruhl, M.: Globally enhanced mercury deposition during the end-Pliensbachian extinction and Toarcian OAE: A link to the Karoo–Ferrar Large Igneous Province, Earth and Planetary Science Letters, 428, 267–280, https://doi.org/10.1016/j.epsl.2015.06.064, http://www.sciencedirect.com/science/article/pii/S0012821X15004276, 2015.

Perez-Fernandez, A., Berninger, U.-N., Mavromatis, V., Von Strandmann, P. P., and Oelkers, E.: Ca and Mg isotope fractionation during the stoichiometric dissolution of dolomite at temperatures from 51 to 126 C and 5 bars CO_2 pressure, Chemical Geology, 467, 76–88, https://doi.org/10.1016/j.chemgeo.2017.07.026, http://www.sciencedirect.com/science/article/pii/S0009254117304254, 2017.

Peucker-Ehrenbrink, B. and Ravizza, G.: The marine osmium isotope record, Terra Nova, 12, 205–219, https://doi.org/10.1046/j.1365-3121.2000.00295.x, https://onlinelibrary.wiley.com/doi/abs/10.1046/j.1365-3121.2000.00295.x, 2000.

Peucker-Ehrenbrink, B., Ravizza, G., and Hofmann, A.: The marine $^{187}Os/^{186}Os$ record of the past 80 million years, Earth and Planetary Science Letters, 130, 155–167, https://doi.org/10.1016/0012-821X(95)00003-U, http://www.sciencedirect.com/science/article/pii/0012821X9500003U, 1995.

Peucker-Ehrenbrink, B., Miller, M. W., Arsouze, T., and Jeandel, C.: Continental bedrock and riverine fluxes of strontium and neodymium isotopes to the oceans, Geochemistry, Geophysics, Geosystems, 11, https://doi.org/10.1029/2009GC002869, https://agupubs.onlinelibrary.wiley.com/doi/abs/10.1029/2009GC002869, 2010.

Phan, T. T., Capo, R. C., Stewart, B. W., Macpherson, G., Rowan, E. L., and Hammack, R. W.: Factors controlling Li concentration and isotopic composition in formation waters and host rocks of Marcellus Shale, Appalachian Basin, Chemical Geology, 420, 162–179, https://doi.org/10.1016/j.chemgeo.2015.11.003, http://www.sciencedirect.com/science/article/pii/S0009254115300954, 2016.

Pistiner, J. S. and Henderson, G. M.: Lithium-isotope fractionation during continental weathering processes, Earth and Planetary Science Letters, 214, 327–339, https://doi.org/10.1016/S0012-821X(03)00348-0, http://www.sciencedirect.com/science/article/pii/S0012821X03003480, 2003.

Pogge von Strandmann, P. A. and Henderson, G. M.: The Li isotope response to mountain uplift, Geology, 43, 67–70, https://doi.org/10.1130/G36162.1, 2015.

Pogge von Strandmann, P. A., Burton, K. W., James, R. H., van Calsteren, P., and Gislason, S. R.: Assessing the role of climate on uranium and lithium isotope behaviour in rivers draining a basaltic terrain, Chemical Geology, 270, 227–239, https://doi.org/10.1016/j.chemgeo.2009.12.002, http://www.sciencedirect.com/science/article/pii/S0009254109004690, 2010.

Pogge von Strandmann, P. A., Burton, K. W., Opfergelt, S., Eiríksdóttir, E. S., Murphy, M. J., Einarsson, A., and Gislason, S. R.: The effect of hydrothermal spring weathering processes and primary productivity on lithium isotopes: Lake Myvatn, Iceland, Chemical Geology, 445, 4–13, https://doi.org/10.1016/j.chemgeo.2016.02.026, http://www.sciencedirect.com/science/article/pii/S0009254116301000, 2016.

Pogge von Strandmann, P. A., Frings, P. J., and Murphy, M. J.: Lithium isotope behaviour during weathering in the Ganges Alluvial Plain, Geochimica et Cosmochimica Acta, 198, 17–31, https://doi.org/10.1016/j.gca.2016.11.017, http://www.sciencedirect.com/science/article/pii/S0016703716306597, 2017.

Pogge von Strandmann, P. A., Hendry, K. R., Hatton, J., and Robinson, L.: The response of magnesium, silicon and calcium isotopes to rapidly uplifting and weathering terrains: South Island, New Zealand, Frontiers in Earth Science, 7, 240, https://doi.org/10.3389/feart.2019.00240, https://www.frontiersin.org/article/10.3389/feart.2019.00240, 2019.

https://doi.org/10.5194/gmd-2020-233
Preprint. Discussion started: 10 August 2020

Racionero-Gómez, B., Sproson, A., Selby, D., Gannoun, A., Gröcke, D., Greenwell, H., and Burton, K. W.: Osmium uptake, distribution, and $^{187}Os/^{188}Os$ and $^{187}Re/^{188}Os$ compositions in Phaeophyceae macroalgae, Fucus vesiculosus: Implications for determining the $^{187}Os/^{188}Os$ composition of seawater, Geochimica et Cosmochimica Acta, 199, 48–57, https://doi.org/10.1016/j.gca.2016.11.033, http://www.sciencedirect.com/science/article/pii/S0016703716306755, 2017.

Richter, E., Hennig, C., Zeimer, U., Weyers, M., Tränkle, G., Reiche, P., Ganschow, S., Uecker, R., and Peters, K.: Freestanding two inch c-plane GaN layers grown on (100) γ-lithium aluminium oxide by hydride vapour phase epitaxy, physica status solidi c, 3, 1439–1443, https://doi.org/10.1002/pssc.200565278, https://onlinelibrary.wiley.com/doi/abs/10.1002/pssc.200565278, 2006.

Rickaby, R., Schrag, D., Zondervan, I., and Riebesell, U.: Growth rate dependence of Sr incorporation during calcification of Emiliania huxleyi, Global biogeochemical cycles, 16, 6–1, https://doi.org/10.1029/2001GB001408, https://agupubs.onlinelibrary.wiley.com/doi/abs/10.1029/2001GB001408, 2002.

Ridgwell, A. and Hargreaves, J.: Regulation of atmospheric CO_2 by deep-sea sediments in an Earth system model, Global Biogeochemical Cycles, 21, https://doi.org/10.1029/2006GB002764, https://agupubs.onlinelibrary.wiley.com/doi/abs/10.1029/2006GB002764, 2007.

Ridgwell, A. and Zeebe, R. E.: The role of the global carbonate cycle in the regulation and evolution of the Earth system, Earth and Planetary Science Letters, 234, 299–315, https://doi.org/10.1016/j.epsl.2005.03.006, http://www.sciencedirect.com/science/article/pii/S0012821X05001883, 2005.

Ridgwell, A., Hargreaves, J., Edwards, N. R., Annan, J., Lenton, T. M., Marsh, R., Yool, A., and Watson, A.: Marine geochemical data assimilation in an efficient Earth System Model of global biogeochemical cycling, Biogeosciences, 4, 87–104, https://doi.org/10.5194/bg-4-87-2007, 2007.

Ridgwell, A. J.: Glacial-interglacial perturbations in the global carbon cycle., Ph.D. thesis, University of East Anglia, 2001.

Rollion-Bard, C., Vigier, N., Meibom, A., Blamart, D., Reynaud, S., Rodolfo-Metalpa, R., Martin, S., and Gattuso, J.-P.: Effect of environmental conditions and skeletal ultrastructure on the Li isotopic composition of scleractinian corals, Earth and Planetary Science Letters, 286, 63–70, https://doi.org/10.1016/j.epsl.2009.06.015, http://www.sciencedirect.com/science/article/pii/S0012821X0900346X, 2009.

Rosner, M., Ball, L., Peucker-Ehrenbrink, B., Blusztajn, J., Bach, W., and Erzinger, J.: A simplified, accurate and fast method for lithium isotope analysis of rocks and fluids, and δ^7Li values of seawater and rock reference materials, Geostandards and Geoanalytical Research, 31, 77–88, https://doi.org/10.1111/j.1751-908X.2007.00843.x, https://onlinelibrary.wiley.com/doi/abs/10.1111/j.1751-908X.2007.00843.x, 2007.

Rudnick, R. L., Tomascak, P. B., Njo, H. B., and Gardner, L. R.: Extreme lithium isotopic fractionation during continental weathering revealed in saprolites from South Carolina, Chemical Geology, 212, 45–57, https://doi.org/10.1016/j.chemgeo.2004.08.008, http://www.sciencedirect.com/science/article/pii/S0009254104002712, 2004.

Rüggeberg, A., Fietzke, J., Liebetrau, V., Eisenhauer, A., Dullo, W.-C., and Freiwald, A.: Stable strontium isotopes ($\delta^{88/86}$Sr) in cold-water corals—a new proxy for reconstruction of intermediate ocean water temperatures, Earth and Planetary Science Letters, 269, 570–575, https://doi.org/10.1016/j.epsl.2008.03.002, http://www.sciencedirect.com/science/article/pii/S0012821X08001763, 2008.

Sharma, M., Papanastassiou, D., and Wasserburg, G.: The concentration and isotopic composition of osmium in the oceans, Geochimica et Cosmochimica Acta, 61, 3287–3299, https://doi.org/10.1016/S0016-7037(97)00210-X, http://www.sciencedirect.com/science/article/pii/S001670379700210X, 1997.

Sharma, M., Rosenberg, E. J., and Butterfield, D. A.: Search for the proverbial mantle osmium sources to the oceans: Hydrothermal alteration of mid-ocean ridge basalt, Geochimica et Cosmochimica Acta, 71, 4655–4667, https://doi.org/10.1016/j.gca.2007.06.062, http://www.sciencedirect.com/science/article/pii/S0016703707004565, 2007.

https://doi.org/10.5194/gmd-2020-233
Preprint. Discussion started: 10 August 2020

Sime, N. G., Christina, L., Tipper, E. T., Tripati, A., Galy, A., and Bickle, M. J.: Interpreting the Ca isotope record of marine biogenic carbonates, Geochimica et Cosmochimica Acta, 71, 3979–3989, https://doi.org/10.1016/j.gca.2007.06.009, http://www.sciencedirect.com/science/article/pii/S0016703707003080, 2007.

Stevenson, E. I., Hermoso, M., Rickaby, R. E., Tyler, J. J., Minoletti, F., Parkinson, I. J., Mokadem, F., and Burton, K. W.: Controls on stable strontium isotope fractionation in coccolithophores with implications for the marine Sr cycle, Geochimica et cosmochimica acta, 128, 225–235, https://doi.org/10.1016/j.gca.2013.11.043, http://www.sciencedirect.com/science/article/pii/S0016703713006820, 2014.

Stoffyn-Egli, P. and Mackenzie, F. T.: Mass balance of dissolved lithium in the oceans, Geochimica et Cosmochimica Acta, 48, 859–872, 1984.

Stoll, H. M. and Schrag, D. P.: Sr/Ca variations in Cretaceous carbonates: relation to productivity and sea level changes, Palaeogeography, Palaeoclimatology, Palaeoecology, 168, 311–336, https://doi.org/10.1016/S0031-0182(01)00205-X, http://www.sciencedirect.com/science/article/pii/S003101820100205X, 2001.

Tang, J., Köhler, S. J., and Dietzel, M.: Sr^{2+}/Ca^{2+} and $^{44}Ca/^{40}Ca$ fractionation during inorganic calcite formation: I. Sr incorporation, Geochimica et Cosmochimica Acta, 72, 3718–3732, https://doi.org/10.1016/j.gca.2008.05.033, http://www.sciencedirect.com/science/article/pii/S0016703708002901, 2008.

Tejada, M. L. G., Suzuki, K., Kuroda, J., Coccioni, R., Mahoney, J. J., Ohkouchi, N., Sakamoto, T., and Tatsumi, Y.: Ontong Java Plateau eruption as a trigger for the early Aptian oceanic anoxic event, Geology, 37, 855–858, https://doi.org/10.1130/G25763A.1, 2009.

Them, T. R., Gill, B. C., Selby, D., Gröcke, D. R., Friedman, R. M., and Owens, J. D.: Evidence for rapid weathering response to climatic warming during the Toarcian Oceanic Anoxic Event, Scientific reports, 7, 1–10, https://doi.org/10.1038/s41598-017-05307-y, 2017.

Tipper, E. T., Galy, A., and Bickle, M. J.: Calcium and magnesium isotope systematics in rivers draining the Himalaya-Tibetan-Plateau region: Lithological or fractionation control?, Geochimica et Cosmochimica Acta, 72, 1057–1075, https://doi.org/10.1016/j.gca.2007.11.029, http://www.sciencedirect.com/science/article/pii/S0016703707006898, 2008.

Tipper, E. T., Schmitt, A.-D., and Gussone, N.: Global Ca cycles: coupling of continental and oceanic processes, in: Calcium Stable Isotope Geochemistry, pp. 173–222, Springer, 2016.

Tomascak, P. B., Carlson, R. W., and Shirey, S. B.: Accurate and precise determination of Li isotopic compositions by multi-collector sector ICP-MS, Chemical Geology, 158, 145–154, https://doi.org/10.1016/S0009-2541(99)00022-4, http://www.sciencedirect.com/science/article/pii/S0009254199000224, 1999.

Turner, S. K. and Ridgwell, A.: Development of a novel empirical framework for interpreting geological carbon isotope excursions, with implications for the rate of carbon injection across the PETM, Earth and Planetary Science Letters, 435, 1–13, https://doi.org/10.1016/j.epsl.2015.11.027, http://www.sciencedirect.com/science/article/pii/S0012821X15007311, 2016.

Vance, D., Teagle, D. A., and Foster, G. L.: Variable Quaternary chemical weathering fluxes and imbalances in marine geochemical budgets, Nature, 458, 493–496, https://doi.org/10.1038/nature07828, 2009.

Veizer, J.: Strontium isotopes in seawater through time, Annual Review of Earth and Planetary Sciences, 17, 141–167, https://doi.org/10.1146/annurev.ea.17.050189.001041, https://doi.org/10.1146/annurev.ea.17.050189.001041, 1989.

Vervoort, P., Adloff, M., Greene, S., and Turner, S. K.: Negative carbon isotope excursions: an interpretive framework, Environmental Research Letters, 14, 085 014, https://doi.org/10.1088/1748-9326/ab3318, 2019.

Vigier, N. and Goddéris, Y.: A new approach for modeling Cenozoic oceanic lithium isotope paleo-variations: the key role of climate, Climate of the Past, 11, 635–645, https://doi.org/10.5194/cp-11-635-2015, https://cp.copernicus.org/articles/11/635/2015/, 2015.

https://doi.org/10.5194/gmd-2020-233
Preprint. Discussion started: 10 August 2020

Vollstaedt, H., Eisenhauer, A., Wallmann, K., Böhm, F., Fietzke, J., Liebetrau, V., Krabbenhöft, A., Farkaš, J., Tomašovỳch, A., Raddatz, J., et al.: The Phanerozoic $\delta^{88/86}$Sr record of seawater: New constraints on past changes in oceanic carbonate fluxes, Geochimica et Cosmochimica Acta, 128, 249–265, https://doi.org/10.1016/j.gca.2013.10.006, http://www.sciencedirect.com/science/article/pii/S0016703713005620, 2014.

Wakaki, S., Obata, H., Tazoe, H., and Ishikawa, T.: Precise and accurate analysis of deep and surface seawater Sr stable isotopic composition by double-spike thermal ionization mass spectrometry, Geochemical Journal, 51, 227–239, https://doi.org/10.2343/geochemj.2.0461, 2017.

Ward, B. A., Wilson, J. D., Death, R. M., Monteiro, F. M., Yool, A., and Ridgwell, A.: EcoGEnIE 1.0: plankton ecology in the cGEnIE Earth system model, Geoscientific Model Development, 11, 4241–4267, https://doi.org/10.5194/gmd-11-4241-2018, 2018.

Weynell, M., Wiechert, U., and Schuessler, J. A.: Lithium isotopes and implications on chemical weathering in the catchment of Lake Donggi Cona, northeastern Tibetan Plateau, Geochimica et Cosmochimica Acta, 213, 155–177, https://doi.org/10.1016/j.gca.2017.06.026, http://www.sciencedirect.com/science/article/pii/S0016703717303757, 2017.

Woodhouse, O., Ravizza, G., Falkner, K. K., Statham, P., and Peucker-Ehrenbrink, B.: Osmium in seawater: vertical profiles of concentration and isotopic composition in the eastern Pacific Ocean, Earth and Planetary Science Letters, 173, 223–233, https://doi.org/10.1016/S0012-821X(99)00233-2, http://www.sciencedirect.com/science/article/pii/S0012821X99002332, 1999.

You, C.-F. and Chan, L.-H.: Precise determination of lithium isotopic composition in low concentration natural samples, Geochimica et Cosmochimica Acta, 60, 909–915, https://doi.org/10.1016/0016-7037(96)00003-8, http://www.sciencedirect.com/science/article/pii/0016703796000038, 1996.

Zhu, P. and Macdougall, J. D.: Calcium isotopes in the marine environment and the oceanic calcium cycle, Geochimica et Cosmochimica Acta, 62, 1691–1698, https://doi.org/10.1016/S0016-7037(98)00110-0, http://www.sciencedirect.com/science/article/pii/S0016703798001100, 1998.